Accepted Manuscript

Novel unsaturated glycyrrhetic acids derivatives: Design, synthesis and anti-inflammatory activity

Bo Li, Shi Cai, Yong-An Yang, Shi-Chao Chen, Rui Chen, Jing-Bo Shi, Xin-Hua Liu, Wen-Jian Tang

PII: S0223-5234(17)30605-0

DOI: 10.1016/j.ejmech.2017.08.002

Reference: EJMECH 9646

To appear in: *European Journal of Medicinal Chemistry*

Received Date: 6 July 2017

Revised Date: 31 July 2017

Accepted Date: 1 August 2017

Please cite this article as: B. Li, S. Cai, Y.-A. Yang, S.-C. Chen, R. Chen, J.-B. Shi, X.-H. Liu, W.-J. Tang, Novel unsaturated glycyrrhetic acids derivatives: Design, synthesis and anti-inflammatory activity, *European Journal of Medicinal Chemistry* (2017), doi: 10.1016/j.ejmech.2017.08.002.

Graphical abstract

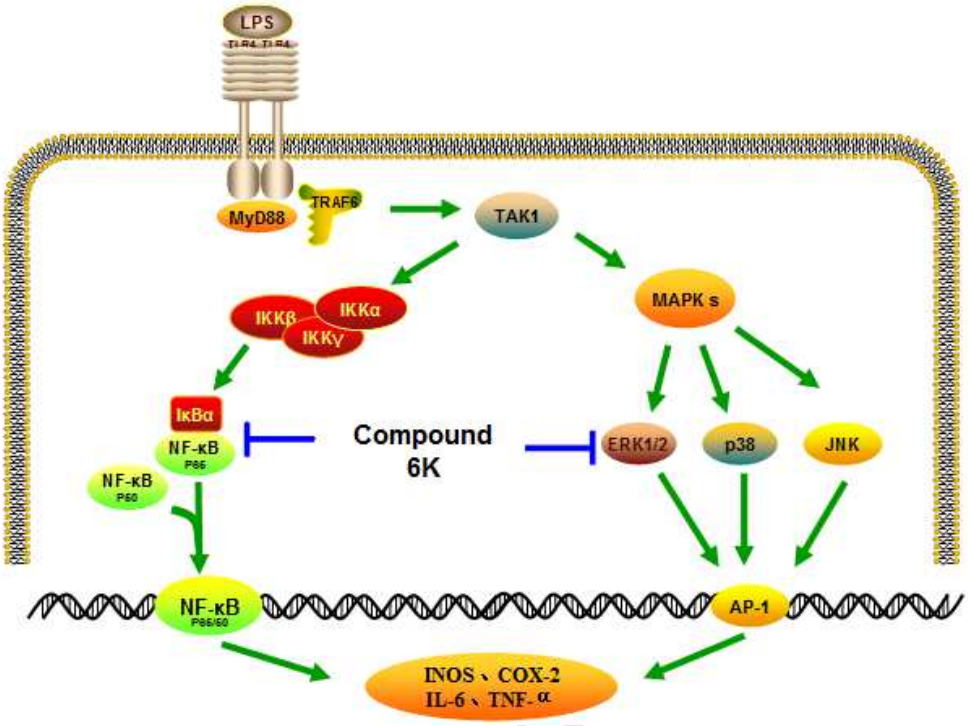

Compound **6k** was much more potent than Glycyrrhetic acid for the anti-inflammatory activity. It could also significantly suppress LPS-induced iNOS and COX-2 expression and IL-6 production through MAPKs and NF-kB signaling pathway.

Novel unsaturated glycyrrhetic acids DERIVATIVES: design, synthesis and anti-inflammatory activity

Bo Li[a,1], Shi Cai[a,1], Yong-An Yang[b], Shi-Chao Chen[a], Rui Chen[a], Jing-Bo Shi[a], Xin-Hua Liu[a,*], Wen-Jian Tang[a,*]

[a] *School of Pharmacy, Anhui Province Key Laboratory of Major Autoimmune Diseases, Anhui Institute of Innovative Drugs, Anhui Medical University, Hefei 230032, China.*
[b] *Elion Nature Biological Technology Co., Ltd, Nanjing 210038, China.*

Abstract: To develop novel anti-inflammatory agents, a series of unsaturated glycyrrhetic acids were designed, synthesized and evaluated for anti-inflammatory activity using RAW264.7 cells. The structure-activity relationship (SAR) of NO inhibitory activity was analyzed. α,β-Unsaturated glycyrrhetic acids showed better activity, among them, compounds **6k** and **6l** with piperazine unit exhibited the most potent nitric oxide (NO) and interleukin-6 (IL-6) inhibitory activity (IC_{50} = 13.3 and 15.5 μM respectively). Furthermore, compound **6k** could also significantly suppress LPS-induced iNOS and COX-2 expression and IL-6 production through MAPKs and NF-kB signaling pathway.

Keywords: glycyrrhetic acid; anti-inflammatory activity; structure-activity relationship; unsaturated carbonyl

*Corresponding author.
Tel. & fax: +86 551 65161115. E-mail: xhliuhx@163.com; ahmupharm@126.com.

[1] B. Li and S. Cai contributed equally to this work.

1. Introduction

Inflammation, the fundamental defense mechanism of the immune system, can protect against injuries caused by harmful stimuli, such as pathogens and poisons. However, the inflammatory process itself may cause tissue damage and lead to numerous diseases and even cancer [1,2]. Nonsteroidal anti-inflammatory drugs (NSAIDs) are therapeutically important in the treatment of pain and inflammation, but the long-term therapy with NSAIDs was soon associated with high incidences of adverse events in the gastrointestinal tract [3,4]. Therefore, the search for novel anti-inflammatory agents, possessing improved pharmaceutical profiles and reduced adverse effects, is still urgently needed. Due to benign therapeutic potency and fewer adverse effects, natural products played a significant part in medicine producing many of the early new molecular entities (NMEs) and nearly half of all approved NMEs [5,6].

Licorice, the roots and rhizomes of *Glycyrrhiza* species, has widely used as a traditional Chinese medicine due to its antibacterial, anti-viral, anti-inflammatory, et al [7–10]. 18β-glycyrrhetic acid (18β-GA, glycyrrhetin) is the main active component with diverse pharmacological activities, including anti-inflammatory, antioxidant, antibacterial, anti-viral and hepatoprotective activities [11–15]. Its anti-inflammatory effect is particularly well-known and has been applied to clinical therapy, because its structure is similar to that of cortisone, a steroid hormone that exerts a strong anti-inflammatory effect [11]. 18β-GA exhibited anti-inflammatory effects by inhibiting the production of inflammatory cytokines and reducing the expression of pro-inflammatory genes [11,16], for example, inhibiting macrophage inflammatory protein (MIP)-1α in a mouse model of acute Propionibacterium acnes-induced inflammatory liver injury [17], inserting the immunomodulatory effects by enhancing DC maturation and modulating Th1/Th2 response in Th1 responses [18]. These results suggested that 18β-GA could be used as a potent anti-inflammatory agent for the treatment and prevention of inflammation-related diseases.

Structural modification of bioactive natural products according to molecular characteristics was an important approach in search for new lead compounds [19–21]. The fact that minor structural changes in triterpenoids can cause extensive changes in biological activity has long intrigued medicinal chemists. The most actively explored

'simple' derivatives of GA, obtained by modification of 3-hydroxy (or 3-oxo) with aminoacids or/and 30-carboxylic groups by esterification, exhibited a higher activity than GA [22–27]. Natural products containing an α,β-unsaturated carbonyl moieties exhibit diverse pharmacological activities, and the most important and widely studied natural compounds include curcumin, chalcone, zerumbone, and so on [28−30]. It was found that the introduction of a 1-en-3-one functionality in several synthetic triterpenoids greatly improved their anti-inflammatory activities [26,27,31,32]. The immunosuppressive effects of the α,β-unsaturated carbonyl moiety on the cells play key role in inflammation, which were partially mediated by their effects on the immune cells specifically on inhibition of pro-inflammatory cytokines expression [30].

Based on the above observations, we proceeded with modification of the GA structure using following strategies: (a) building up an α,β-unsaturated carboxylic acid moiety at C-30 in ring E of GA, namely glycyrrhetenoic acid (**5**); (b) converting C-32 carboxyl group to an ester or amide functionality (Fig. 1). Thus, nineteen compounds were synthesized and evaluated for their anti-inflammatory activity with lipopolysaccharide (LPS)-induced RAW264.7 cells through inhibiting NO production. Further, the most potent compounds **6k** and **6l** with piperazine moiety were used study the preliminary mechanism of anti-inflammatory action.

(Fig. 1)

2. Results and discussion

2.1. Chemistry

The introduction of an α,β-unsaturated carbonyl in natural products could improve their pharmacological activities [30]. The preparation of the key intermediate **5** containing an α,β-unsaturated carbonyl unit was outlined in Scheme 1. Compound **2** was prepared by treating the acetate of glycyrrhetic acid with ethyl chloroformate and subsequently reducing it with $NaBH_4$ as previously described [33]. Compound **2** was oxidized with pyridinium chlorochromate (PCC) in CH_2Cl_2 to obtain aldehyde **3**. *Z*-α,β-unsaturated carbonyl compound **5** was obtained from Wittig-Horner reaction of aldehyde **3** and next hydrolysis reaction.

(Scheme 1)

According to recent review [34], elongation of the GA carbohydrate chains or introduction of amino acids or heterocyclic fragments has previously been shown to significantly affect the anti-inflammatory activities. In this regard, we chose to explore whether chemical modifications of the C-30 carboxylic acid affect the anti-inflammatory activity. Consequently, we synthesized a series of glycyrrhetenoic acid derivatives **6a**−**6q** and **7a**−**7b** containing an alkyl, aromatic ring or heterocycle residue with amide bond or ester bond (Scheme 2 and 3).

(Scheme 2)

(Scheme 3)

2.2. Crystal structure analysis

The structure of compound **6b** was determined by X-ray crystallography. As shown in Fig. 2, the absolute configuration of compound **6b** was determined using CuKα radiation (λ = 1.54184 Å), such as C3(*S*), C5(*R*), C8(*R*), C9(*R*), C10(*S*), C17(*R*), C18(*R*) and C20(*S*) (Scheme 1). In compound **6b**, the *cis* D/E stereochemistry was consistent with that of natural 18β-GA. Crystallographic data (excluding structure factors) for the structures have been deposited in the Cambridge Crystallographic Data Center as supplementary publication No. CCDC 1418308.

(Fig. 2)

2.3. Cytotoxicity of glycyrrhetin derivatives

To investigate whether the inflammatory inhibitory activities of glycyrrhetin derivatives were related to cell viability, their cytotoxicity were evaluated by MTT assay in RAW264.7 cells. As shown in Table 1, compounds GA, **5**, **6a-p**, **7a-b** and LPS at the test concentrations (40 μM or 20 μM for low solubility) had no obviously cytotoxicity in RAW264.7 cells, and the relative cell viabilities of the treated cells were all more than 90%. These results indicated that the non-toxic concentrations

were further used in subsequent experiment processes.

(Table 1)

2.4. Inhibition of NO production in (LPS)-stimulated RAW264.7 cells

NO is a significant pro-inflammatory mediator. Excessive production of NO was found to be associated with the pathogenesis of inflammation diseases. It is generally accepted that NO inhibitors may offer potential opportunity to identify new therapeutic method for the inflammatory diseases [35,36]. To evaluate the anti-inflammatory effect of glycyrrhetin derivatives, Griess reagent was used to detect the level of lipopolysaccharide (LPS)-induced NO release in RAW264.7 cells. As shown in Fig. 3, LPS treatment caused significant increase of NO release compared to blank, after glycyrrhetin derivatives treatment, the increase of LPS-induced NO release could be alleviated in RAW264.7 cells. Among them, compounds **5**, **6a-6e**, **6k**, **6l** and **6n** significantly alleviated the increase of LPS-induced NO release. As expected [30], glycyrrhetenoic acid (compound **5**) with α,β-unsaturated carbonyl moiety exhibited better NO inhibitory activity than glycyrrhetic acid. The order of NO inhibitory activity of 32-substituted glycyrrhetenoic acid **5** was: (i) heterocycle amide (**6k**, **6l**, **6n** except for **6m**) > linear alkyl amide (**6a-6e**; **6d**, **6e** at 20μM) > branched alkyl amide (**6f**; **6g** at 20μM); (ii) amide > ester (**6i** > **7b**); (iii) no significant NO inhibitory activity for compounds with aromatic ring (**6i**, **6j**, **6o**, **7b**). Overall, glycyrrhetin derivatives displayed preferable anti-inflammatory activity, particularly, compounds **6k** and **6l** with piperazine moiety exhibited the most potent inhibitory activity and their NO inhibition rate exceeded 70% at the concentration of 40 μM. These results could be very useful for our future SAR study.

(Fig. 3)

*2.5. Compound **6k** and **6l** inhibited IL-6 and TNF-α production in RAW264.7 cells*

LPS-induced activated macrophages produce a variety of inflammatory cytokines, including tumor necrosis factor (TNF-α), interleukins (ILs), and inflammatory mediators nitric oxide (NO), prostaglandins (PGs), which have a host defensive effect during inflammatory situations and also maintain normal cellular conditions [37]. To

further evaluate the effects of compounds **6k** and **6l** on LPS-induced IL-6 and TNF-α production, RAW264.7 cells were cultured with LPS (1 μg/mL) in the presence of compounds **6k** and **6l** for 24 h, and the levels of IL-6 and TNF-α in the supernatant were determined by ELISA. As shown in Fig. 4, the LPS stimulation significantly elevated the productions of TNF-α and IL-6 compared to the normally basal level of the cytokines in macrophages. Treatment with compounds **6k** and **6l** inhibited the LPS-induced production of IL-6 and TNF-α in a concentration-dependent manner (Figs. 4A and 4B). After compounds **6k** and **6l** treatment, the augmented levels of IL-6 by LPS were more markedly decreased than that of TNF-α. Data analysis showed that IC_{50} values of inhibitory effect of compounds **6k** and **6l** on IL-6 were 13.3 μM and 15.5 μM respectively. These results showed that compounds **6k** and **6l** certainly attenuate an excessive immune reaction in RAW 264.7 macrophages by blocking the increase of pro-inflammatory cytokines stimulated by LPS. Thus, compound **6k** was selected to further explore the mechanisms of the anti-inflammatory effect.

(Fig. 4)

*2.6. Compound **6k** inhibited LPS-induced inflammatory mediators in RAW264.7 cells*

The pro-inflammatory mediators (NO, PGE_2) play important roles in inflammation-related diseases, which are also importantly related to the modulation of iNOS and COX-2 expression [38]. To evaluate the impact of compound **6k** treatment on protein expression in LPS-induced RAW 264.7 cells, COX-2 and nitric oxide synthase (iNOS) protein levels were analyzed after exposure to LPS for 24 h in presence or absence of compound **6k** (10, 20, or 40 μM) by Western blot. Bay 11-7082 (20 μM) was used as a positive control. The results showed that LPS (1 μg/mL) stimulation could markedly increase COX-2 and iNOS protein expression. Pretreatment with compound **6k** significantly inhibited LPS-induced COX-2 and iNOS production by 55.6% and 76.9% at 40 μM respectively (Fig. 5). Also, compound **6k** inhibited COX-2 and iNOS protein expression in LPS-induced cells in a dose-dependent manner (Fig. 5). These preliminary results demonstrated that compound **6k** may participate in signaling pathways activated by LPS in macrophages.

(Fig. 5)

*2.7. Compound **6k** inhibits LPS-induced NF-κB activation in RAW264.7 cells*

Stimulation with LPS leads to the activation of NF-κB, which is a well-known transcription factor that positively regulates inflammatory genes including iNOS and COX-2 in many human diseases [39]. NF-κB activation is controlled by phosphorylation and degradation of IκB-α, a cognate regulatory subunit of NF-κB [40]. Therefore, western blotting and Immunofluorescence were used to examine the effects of compound **6k** on LPS-induced transcriptional activity of NF-κB in LPS-stimulated RAW 264.7 cells. As shown in Fig. 6A, LPS significantly increased the levels of phosphorylated NF-κB p65, IκBα and compound **6k** treatment displayed a concentration-dependent inhibition of LPS-induced NF-κB transcriptional activity after 30 min of LPS exposure. Furthermore, the nuclear translocation of NF-κB was examined in LPS-stimulated RAW264.7 cells. Immunofluorescence analysis showed that LPS stimulation increased nuclear translocation of the p65 subunit, and compound **6k** clearly inhibited NF-κB p65 nuclear translocation from the cytosol to the nucleus (Fig. 6B). Taken together, we suggest that compound **6k** could regulate the expression of pro-inflammatory proteins through inhibition of NF-κB signaling pathways.

(Fig. 6)

*2.8. Compound **6k** suppresses LPS-induced MAPK activation in RAW264.7 cells*

The mitogen-activated protein kinases (MAPKs) are a family of signal transduction proteins that include extracellular signal-regulated kinase (ERK), c-Jun N-terminal kinases (JNK), and the p38 isoform (p38), which are classical pathways that modulate immune-mediated inflammatory responses and cellular activities involved in cell survival and apoptosis through the corresponding signaling cascades [41–43]. Activated MAPKs modify the phosphorylation on the threonine/tyrosine motif, accelerating iNOS, COX-2, and pro-inflammatory cytokine expression in activated macrophages [42,44]. To determine the effects of compound **6k** on the LPS-induced phosphorylation of MAPKs, the expression of ERK, JNK, and p38 was examined. As

expected (Fig. 7), levels of phosphorylation of p38, JNK, and ERK were increased after LPS-stimulated for 30 min. Compound **6k** suppressed LPS-induced phosphorylation of ERK in 40 μM, but had little effect on phosphorylation of JNK or p38 in RAW264.7 cells. These results suggested that the anti-inflammatory activity of compound **6k** might be associated with its negative effects on ERK activation.

(Fig. 7)

3. Conclusion

In conclusion, based on the structure characteristics, a series of glycyrrhetic acid derivatives as anti-inflammatory agents were designed and synthesized. *In vitro* bioassays showed that title compounds could be alleviated the increase of LPS-induced NO release in RAW264.7 cells. The order of NO inhibitory activity was: (i) compound **5** with α,β-unsaturated carbonyl moiety > glycyrrhetic acid; (ii) heterocycle amide (**6k**, **6l**, **6n**) > linear alkyl amide (**6a-6c**) > branched alkyl amide (**6f**); (iii) amide > ester (**6i** > **7b**). Compounds **6k** and **6l** with piperazine moiety exhibited the most potent nitric oxide (NO) and interleukin-6 (IL-6) inhibitory activity (IC_{50} = 13.3 μM and 15.5 μM for IC_{50} values on IL-6 inhibition respectively). Western blotting and immunofluorescence showed that compounds **6k** reduced decreased the expression of iNOS, COX-2, and MAPKs, as well as activation of NF-κB in LPS-stimulated RAW264.7 cells. Taken together, compounds **6k** exerted its anti-inflammatory activity through inhibition of NO generation as a result of inhibiting NF-κB and MAPKs-related inflammatory signaling pathways. These results could be very useful for the SAR study in the future.

4. Experimental section

4.1. Chemistry

All reagents were purchased from commercial sources and were used without further purification. Melting points (uncorrected) were determined on a XT4MP apparatus (Taike Corp., Beijing, China). ^{1}H NMR and ^{13}C NMR spectra were recorded on Bruker AV-400 or AV-300 MHz instruments in $CDCl_3$. Chemical shifts are reported in parts per million (δ) downfield from the signal of tetramethylsilane (TMS) as internal

standards. Coupling constants are reported in Hz. The multiplicity is defined by *s* (singlet), *d* (doublet), *t* (triplet), or *m* (multiplet). High resolution mass spectra (HRMS) were obtained on an Agilent 1260-6221 TOF mass spectrometry. Column and thin-layer chromatography (CC and TLC, resp.) were performed on silica gel (200-300 mesh) and silica gel GF_{254} (Qingdao Marine Chemical Factory) respectively.

*4.2. The synthesis of title compound glycyrrhetenoic acid **5***

*4.2.1. (3β,20β)-3-Acetoxyl-11-oxo-olean-12-en-29-dehyde (**3**)*

This compound was prepared as previously reported [33]: A solution of glycyrrhetic acid (2.5 g, 5.3 mmol) in pyridine (10 mL) THF (20 mL) was added acetic anhydride (1.0 mL, 11 mmol) over 30 min, and the mixture was stirred and heated to reflux for 2 h. The reaction solution was evaporated *in vacuum*, and the residue was recrystallized from ethanol to obtain glycyrrhetic acid acetate (**1**). Ethyl chloroformate (2 mL, 21 mmol) was dropped to a solution of **1** (2.26 g, 4.4 mmol) and Et_3N (2 mL) in THF (10 mL) over 30 min at −5 °C, and the mixture was stirred for 30 min at the same temperature. The precipitate was filtered and washed with THF, and the combined filtrates were added over 30 min to a solution of $NaBH_4$ (1.0 g, 25 mmol) in H_2O (5 mL) in ice bath. Then the reaction mixture was stirred at room temperature for 4 h and acidified with diluted HCl to pH 5−6, the reaction mixture was twice extracted with EtOAc. The organic phase was washed twice with water, then dried over anhydrous Na_2SO_4, filtered, and concentrated under the reduced pressure. The residue was recrystallized from ethanol to obtain compound **2** (white crystal powder, 1.46 g, yield 55% for two-step reaction, no purification for the next reaction).

A solution of **2** (1.45 g, 2.9 mmol) in CH_2Cl_2 (30 mL) was added pyridinium chlorochromate (PCC, 1.50 g, 7.0 mmol) in an ice bath for 1 h, and the mixture was stirred for 2 h at room temperature. The precipitate was filtered over a celite pad and washed with EtOAc, and the combined filtrate was washed twice with water, then dried over anhydrous Na_2SO_4, filtered, and concentrated under the reduced pressure. The residue was purified by flash column chromatography (petroleum/EtOAc = 1/1, v/v) to obtain aldehyde **3** as white powder (0.52 g, 47%), which was used directly for the next step reaction [45]. M.p. 235–238 °C; ^{1}H-NMR (300 MHz, $CDCl_3$), δ (ppm): 9.42 (s, 1H, O=CH), 5.67 (s, 1H, H-12), 4.52 (dd, 1H, J = 11.3, 5.2 Hz, H-3), 2.80 (m,

1H, H-18), 2.36 (s, 1H, H-9), 2.05 (s, 3H, OAc), 1.39 (s, 3H), 1.16 (s, 3H), 1.13 (s, 3H), 0.98 (s, 3H), 0.88 (s, 2×3H), 0.82 (s, 3H).

*4.2.2. Ethyl (3β,20β)-3-acetoxyl-11-oxo-olean-12,30(31)-dien-32-oate (**4**)*

This compound was obtained from Wittig-Horner reaction of compound **3** [46]. Triethyl phosphonoacetate (1.40 g, 6.0 mmol) was dropwise added to a stirred mixture of 80% NaH (250 mg, 6.0 mmol) in dry THF (100 mL) over 30 min in nitrogen at 0–5°C. After addition of triethyl phosphonoacetate is completed, the mixture is stirred for 1 h at 0–5°C. To the reaction mixture was dropwise added a solution of compound **3** (2.50 g, 5.0 mmol) in THF (30 mL) over 30 min in an ice bath, the mixture was then stirred at room temperature for 2 h. The precipitate was filtered and washed with EtOAc, and the combined filtrate was washed twice with water, then dried over anhydrous Na_2SO_4, filtered, and concentrated under the reduced pressure. The residue was recrystallized from ethanol to obtain compound **4** as white crystal powder (1.83 g, 64%), m.p. 254–257 °C; ^{1}H-NMR (600 MHz, $CDCl_3$), δ (ppm): 6.89 (d, 1H, J = 16.2 Hz, H-30), 5.79 (d, 1H, J = 16.2 Hz, H-31), 5.63 (s, 1H, H-12), 4.52 (m, 1H, 3-H), 4.21 (q, 1H, J = 7.1 Hz), 2.80 (m, 1H, H-18), 2.36 (s, 1H, H-9), 2.05 (s, 3H, Ac), 1.37 (s, 3H), 1.31 (q, 1H, J = 7.1 Hz), 1.16 (s, 3H), 1.12 (s, 3H), 1.02 (s, 3H), 0.88 (s, 6H), 0.82 (s, 3H); ^{13}C-NMR (125 MHz, $CDCl_3$), δ (ppm): 200.2 (C-11), 171.2 (Ac-C=O), 169.7 (C-13), 167.1 (C=O), 155.7 (C-30), 128.6 (C-12), 120.4 (C-31), 81.8 (C-3), 62.0 (C-9), 60.6 (OCH_2), 55.3 (C-9), 47.6 (C-5), 45.7 (C-18), 43.5, 43.0, 39.0, 38.3, 38.0, 37.2, 37.0, 33.4, 32.9, 32.5, 31.1, 28.7, 28.3, 26.65, 26.60, 23.8, 23.7, 21.5, 18.9, 17.6, 16.9, 16.6, 14.5 (CH_2CH_3). TOF-HRMS: *m/z* $[M + Na]^+$ calcd for$C_{36}H_{54}NaO_5$: 589.3863; found: 589.3862.

*4.2.3. (3β,20β)-3-Hydroxyl-11-oxo-olean-12,30(31)-dien-32-oic acid (**5**)*

A NaOH solution (50 mL, 5%) was added to a solution of **4** (1.80 g, 3.2 mmol) in EtOH/$CHCl_3$ mixed solvent (5/1, 60 mL) at room temperature, and the mixture was stirred for 2 h. The reaction mixture was acidified with diluted HCl to pH 4−5, extracted twice with $CHCl_3$. The organic phase was washed with water and brine solution, then dried over anhydrous Na_2SO_4, filtered, and concentrated under the reduced pressure. Compound **5** was obtained as white powder (1.44 g, 91%), m.p. 259–262°C; ^{1}H-NMR (300 MHz, $CDCl_3$), δ (ppm): 7.00 (d, 1H, J = 16.2 Hz, H-30), 5.82 (d, 1H, J = 16.2 Hz, H-31), 5.66 (s, 1H, H-12), 3.73 (q, 2H, J = 7.0 Hz), 3.24 (m,

1H, H-3), 2.79 (m, 1H, H-18), 2.36 (s, 1H, H-9), 2.34 (s, 1H, H-9), 1.38 (s, 3H), 1.13 (s, 3H), 1.12 (s, 3H), 1.00 (s, 3H), 1.01 (s, 3H), 0.81 (s, 3H), 0.80 (s, 3H); ^{13}C-NMR (75 MHz, $CDCl_3$), δ (ppm): 200.3 (C-11), 170.4 (C-13), 169.5 (C-32), 157.9 (C-30), 128.3 (C-12), 119.4 (C-31), 78.8 (C-3), 61.8 (C-9), 58.4 (C-22), 54.9 (C-5), 47.4 (C-18), 45.4, 43.3, 42.8, 39.1 (2C), 38.0, 37.1, 36.7, 32.7, 32.2, 30.7, 28.4, 28.0, 26.4, 26.3, 23.5, 18.6, 18.4, 17.4, 16.3, 15.5. TOF-HRMS: *m/z* $[M + H]^+$ calcd for $C_{32}H_{49}O_4$: 497.3625; found: 497.3628.

*4.3. General procedures for converting the carboxylic acid to an amide for compounds **6a–6p**.*

To a solution of glycyrrhetenoic acid **5** (0.50 mmol, 250 mg), EDC·HCl (230 mg, 1.2 mmol), HOBt (165 mg, 1.2 mmol) and corresponding amine (1.0 mmol, 2 equiv.) in CH_2Cl_2 (20 mL), was added NEt_3 (2.0 mmol, 0.3 mL). The reaction mixture was stirred overnight at room temperature. The reaction mixture was added to ice-water (50 mL) and the two layers of the reaction mixture were subsequently separated. The organic layer was washed twice with water and then dried over anhydrous Na_2SO_4. The solvent was evaporated to yield a residue, which was crystallized from ethanol to obtain the amides **6a**–**6p**.

*4.3.1. N-Methyl (3β,20β)-3-hydroxyl-11-oxo-olean-12,30(31)-dien-32-amide (**6a**).* White powder, yield, 67%; m.p. 269–271°C; ^{1}H-NMR (300 MHz, $CDCl_3$), δ (ppm): 6.78 (d, 1H, *J* = 15.8 Hz, H-30), 5.68 (d, 1H, *J* = 15.8 Hz, H-31), 5.55 (s, 1H, H-12), 3.23 (m, 1H, H-3), 2.90 (d, 3H, *J* = 4.9 Hz, NCH_3), 2.79 (m, 1H, H-18), 2.34 (s, 1H, H-9), 1.38 (s, 3H), 1.13 (s, 3H), 1.12 (s, 3H), 1.00 (s, 3H), 1.01 (s, 3H), 0.81 (s, 3H), 0.80 (s, 3H); ^{13}C-NMR (75 MHz, $CDCl_3$), δ (ppm): 200.2 (C-11), 169.6 (C-13), 166.5 (C-32), 150.9 (C-30), 128.2 (C-12), 121.9 (C-31), 78.7 (C-3), 61.8 (C-9), 54.9 (C-5), 47.2 (C-18), 45.4 (C-8), 43.3, 42.6, 39.1 (2C), 37.4, 37.1, 36.8, 35.8, 33.6, 32.7, 31.2, 28.4, 28.1, 27.3, 26.44, 26.36, 23.5, 18.6, 17.4, 16.4, 16.3, 15.5. TOF-HRMS: *m/z* $[M + H]^+$ calcd for $C_{33}H_{52}NO_3$: 510.3942; found: 510.3940.

*4.3.2. N,N-Dimethyl (3β,20β)-3-hydroxyl-11-oxo-olean-12,30(31)-dien-32-amide (**6b**).* White powder, yield, 70%; m.p. 265–268°C; ^{1}H-NMR (300 MHz, $CDCl_3$), δ (ppm): 6.78 (d, 1H, J = 15.8 Hz, H-30), 5.68 (d, 1H, J = 15.8 Hz, H-31), 5.55 (s, 1H, H-12), 3.23 (m, 1H, H-3), 2.90 (s, 2×3H, NCH_3), 2.79 (m, 1H, H-18), 2.34 (s, 1H, H-9), 1.38 (s, 3H), 1.13 (s, 3H), 1.12 (s, 3H), 1.00 (s, 3H), 1.01 (s, 3H), 0.81 (s, 3H), 0.80 (s, 3H); ^{13}C-NMR (75 MHz, $CDCl_3$), δ(ppm): 200.2 (C-11), 169.6 (C-13), 166.5 (C-32), 150.9 (C-30), 128.2 (C-12), 121.9 (C-31), 78.7 (C-3), 61.8 (C-9), 54.9 (C-5), 47.4 (C-18), 45.4 (C-8), 43.3, 42.8, 39.1 (2C), 37.7, 37.5, 37.1, 36.8, 33.7, 32.8, 32.3, 31.2, 28.5, 28.1, 27.3, 26.44, 26.39, 23.1, 18.7, 17.4, 16.4, 16.3, 15.5. TOF-HRMS: *m/z* $[M + H]^+$ calcd for $C_{34}H_{54}NO_3$: 524.4098; found: 524.4096.

*4.3.3. N-Ethyl (3β,20β)-3-hydroxyl-11-oxo-olean-12,30(31)-dien-32-amide (**6c**).* White powder, yield, 60%; m.p. 265–269°C; ^{1}H-NMR (300 MHz, $CDCl_3$), δ (ppm): 6.92 (d, 1H, J = 15.6 Hz, H-30), 6.07 (d, 1H, J = 15.6 Hz, H-31), 5.55 (s, 1H, H-12), 4.62 (m, 2H), 3.14 (m, 2H, CH_2CH_3), 2.77 (m, 1H, H-18), 2.34 (s, 1H, H-9), 1.38 (s, 3H), 1.13 (s, 3H), 1.12 (s, 3H), 1.00 (s, 3H), 1.01 (s, 3H), 0.81 (s, 3H), 0.80 (s, 3H); ^{13}C-NMR (75 MHz, $CDCl_3$), δ (ppm): 200.3 (C-11), 170.0 (C-13), 165.7 (C-32), 150.9 (C-30), 128.2 (C-12), 122.1 (C-31), 78.7 (C-3), 61.8 (C-9), 54.9 (C-5), 53.4 (CH_2CH_3), 47.2 (C-18), 45.4 (C-8), 43.3, 42.5, 39.1 (2C), 37.4, 37.1, 36.8, 34.5, 33.7, 32.7, 31.2, 28.5, 28.1, 27.3, 26.43, 26.36, 23.5, 18.6, 17.4, 16.4, 15.6, 14.8 (CH_2CH_3). TOF-HRMS: *m/z* $[M + H]^+$ calcd for $C_{34}H_{53}NaNO_3$: 546.3918; found: 546.3916.

*4.3.4. N-(2-Hydroxyl)ethyl (3β,20β)-3-hydroxyl-11-oxo-olean-12,30(31)-dien-32-amide (**6d**).* White powder, yield, 50%; m.p. 278–281°C; ^{1}H-NMR (300 MHz, $CDCl_3$), δ (ppm): 6.82 (d, 1H, J = 15.7 Hz, H-30), 5.77 (d, 1H, J = 15.5 Hz, H-31), 5.59 (s, 1H, H-12), 3.78 (m, 2H, CH_2O), 3.52 (m, 2H, NCH_2), 3.23 (m, 1H, H-3), 2.79 (m, 1H, H-18), 2.34 (s, 1H, H-9), 1.38 (s, 3H), 1.13 (s, 3H), 1.12 (s, 3H), 1.00 (s, 3H), 1.01 (s, 3H), 0.81 (s, 3H),

0.80 (s, 3H); ^{13}C-NMR (75 MHz, $CDCl_3$), δ (ppm): 200.7 (C-11), 170.6 (C-13), 166.6 (C-32), 151.4 (C-30), 128.0 (C-12), 122.0 (C-31), 78.7 (C-3), 66.9 (CH_2O), 61.8 (C-9), 54.9 (C-5), 47.9 (NCH_2), 47.1 (C-18), 45.5 (C-8), 43.3, 42.2, 39.1 (2C), 37.5, 37.1, 37.0, 33.7, 32.7, 32.3, 31.2, 28.5, 28.1, 27.2, 26.40, 26.34, 23.5, 18.7, 17.4, 16.4, 15.6. TOF-HRMS: *m/z* $[M + H]^+$ calcd for $C_{34}H_{54}NO_4$: 540.4047; found: 540.4045.

*4.3.5. N-(2-Hydroxyl)propyl (3β,20β)-3-hydroxyl-11-oxo-olean-12,30(31)-dien-32-amide (**6e**).* White powder, yield, 60%; m.p. 280–284°C; ^{1}H-NMR (300 MHz, $CDCl_3$), δ (ppm): 6.78 (d, 1H, *J* = 15.8 Hz, H-30), 6.57 (d, 1H, NH), 5.80 (d, 1H, *J* = 15.8 Hz, H-31), 5.62 (s, 1H, H-17), 1.13 (s, 3H), 1.12 (s, 3H), 1.00 (s, 3H), 1.01 (s, 3H), 0.81 (s, 3H), 0.80 (s, 3H); ^{13}C-NMR (75 MHz, $CDCl_3$), δ (ppm): 200.7 (C-11), 170.6 (C-13), 166.6 (C-32), 151.4 (C-30), 128.0 (C-12), 122.0 (C-31), 78.7 (C-3), 66.9 (OCH_2), 61.8 (C-9), 54.9 (C-5), 47.9 (NCH_2), 47.1 (C-18), 45.5 (C-8), 43.3 (C-14), 42.2, 39.1 (2C), 37.5, 37.1, 36.8, 33.7, 32.7, 32.2, 31.2, 28.5, 28.1, 27.2, 26.4, 26.3, 23.5, 23.1, 18.6, 17.0, 16.3, 15.6. TOF-HRMS: *m/z [*$M + H]^+$ calcd for $C_{35}H_{56}NO_4$: 554.4204; found: 554.4202.

*4.3.6. N-Isopropyl (3β,20β)-3-hydroxyl-11-oxo-olean-12,30(31)-dien-32-amide (**6f**).* White powder, yield, 86%; m.p. 254–257°C; ^{1}H-NMR (300 MHz, $CDCl_3$), δ (ppm): 6.78 (d, 1H, *J* = 15.8 Hz, H-30), 5.68 (d, 1H, *J* = 15.8 Hz, H-31), 5.61 (s, 1H, H-12), 5.58 (d, 1H, NH), 3.23 (m, 1H, H-3), 2.90 (m, 1H, *i*-Pr-CH), 2.79 (m, 1H, H-18), 2.34 (s, 1H, H-9), 1.13 (s, 3H), 1.12 (s, 3H), 1.00 (s, 3H), 1.01 (s, 3H), 0.81 (s, 3H), 0.80 (s, 3H); ^{13}C-NMR (75 MHz, $CDCl_3$), δ (ppm): 200.4 (C-11), 170.2 (C-13), 165.0 (C-32), 150.9 (C-30), 128.2 (C-12), 122.3 (C-31), 78.7 (C-3), 61.9 (C-9), 55.0 (C-5), 47.2 (C-18), 45.5 (C-8), 43.3, 42.8, 42.2, 39.2 (2C), 37.4, 37.1, 36.8, 33.7, 32.7, 32.3, 31.2, 28.5, 28.1, 27.3, 26.42, 26.36, 23.5, 22.8 (2C), 18.7, 17.4, 16.3, 15.5. TOF-HRMS: *m/z* $[M + H]^+$ calcd for $C_{35}H_{56}NO_3$: 538.4255; found: 538.4254.

4.3.7. N,N-Diisopropyl (3β,20β)-3-hydroxyl-11-oxo-olean-12,30(31)-dien-32-amide

(6g). White powder, 76%; m.p. 264–268°C; ^{1}H-NMR (300 MHz, $CDCl_3$), δ (ppm): 6.78 (d, 1H, J = 15.8 Hz, H-30), 5.68 (d, 1H, J =15.8 Hz, H-31), 5.55 (s, 1H, H-12), 3.94 (s, 1H, NH), 3.23 (m, 1H, H-3), 2.90 (m, 2H, H-33), 2.79 (m, 1H, H-18), 2.34 (s, 1H, H-9), 1.38 (s, 3H), 1.13 (s, 3H), 1.12 (s, 3H), 1.00 (s, 3H), 1.01 (s, 3H), 0.81 (s, 3H), 0.80 (s, 3H); ^{13}C-NMR (75 MHz, $CDCl_3$), δ (ppm): 200.2 (C-11), 169.6 (C-13), 166.5 (C-32), 150.9 (C-30), 128.2 (C-12), 121.9 (C-31), 78.7 (C-3), 61.8 (C-9), 54.9 (C-5), 47.4 (C-18), 45.4 (C-8), 43.3, 43.0 (2C), 42.7, 39.1 (2C), 37.6, 37.4, 37.1, 36.7, 33.6, 32.2, 31.2, 28.4, 28.1, 27.3, 26.4, 26.4, 23.5, 23.1 (4C), 18.7, 17.5, 16.3, 15.5. TOF-HRMS: *m/z* $[M + H]^+$ calcd for $C_{38}H_{62}NO_3$: 580.4724; found: 580.4726.

4.3.8. N-(3-Chloro)propyl (3β,20β)-3-hydroxyl-11-oxo-olean-12,30(31)-dien-32-amide ***(6h)***. White powder, yield, 67%; m.p. 243–246°C; ^{1}H-NMR (300 MHz, $CDCl_3$), δ (ppm): 6.78 (d, 1H, J = 15.8 Hz, H-30), 5.68 (d, 1H, J =15.8 Hz, H-31), 5.55 (s, 1H, H-12), 3.62 (t, 2H, J = 6.8 Hz, $ClCH_2$), 3.50 (m, 2H), 3.23 (m, 1H, H-3), 2.79 (m, 1H, H-18), 2.34 (s, 1H, H-9), 2.07 (m, 4H), 1.38 (s, 3H), 1.13 (s, 3H), 1.12 (s, 3H), 1.00 (s, 3H), 1.01 (s, 3H), 0.81 (s, 3H), 0.80 (s, 3H); ^{13}C-NMR (75 MHz, $CDCl_3$), δ (ppm): 200.4 (C-11), 170.1 (C-13), 166.2 (C-32), 151.5 (C-30), 128.2 (C-12), 121.9 (C-31), 78.7 (C-3), 61.9 (C-9), 54.9 (C-5), 47.2 (C-18), 45.4 (C-8), 43.3, 42.6, 39.1 (2C), 37.5, 37.1 (2C), 36.8, 33.6, 32.7, 32.3, 32.2, 31.2, 29.7, 28.5, 28.1, 27.3, 26.42, 26.38, 23.5, 18.7, 17.4, 16.3, 15.5. TOF-HRMS: *m/z* $[M + H]^+$ calcd for $C_{35}H_{55}ClNO_3$: 572.3865; found: 572.3863.

4.3.9. N-(2-Phenyl)ethyl (3β,20β)-3-hydroxyl-11-oxo-olean-12,30(31)-dien-32-amide ***(6i)***. White powder, yield, 50%; m.p. 287–291°C; ^{1}H-NMR (300 MHz, $CDCl_3$), δ (ppm): 7.33 (m, 2H, H-Ar), 7.23 (m, 3H, H-Ar), 6.80 (d, 1H, J = 15.8 Hz, H-30), 5.65 (d, 1H, J = 15.8 Hz, H-31), 5.57 (s, 1H, H-12), 3.61 (m, 2H, NCH_2), 3.23 (m, 1H, H-3), 2.88 (t, 2H, J = 7.1 Hz, PhCH_2), 2.80 (m, 1H, H-18), 2.34 (s, 1H, H-9), 1.38 (s, 3H), 1.13 (s, 3H), 1.12 (s, 3H), 1.00 (s, 3H), 1.01 (s, 3H), 0.81 (s, 3H), 0.80 (s, 3H); ^{13}C-NMR (75 MHz, $CDCl_3$), δ (ppm): 200.2 (C-11), 169.8 (C-13), 165.8 (C-32),

151.2 (C-30), 138.0 (C-Ar), 128.7 (2C-Ar), 128.6 (2C-Ar), 128.2 (C-12), 126.5 (C-Ar), 122.0 (C-31), 78.7 (C-3), 61.8 (C-9), 54.9 (C-5), 47.1 (C-18), 45.4 (C-8), 43.3, 40.8, 39.1 (2C), 37.4, 37.1, 36.8, 35.7, 33.6, 32.7, 32.3 (2C), 31.1, 28.5, 28.1, 27.3, 26.44, 26.38, 23.5, 18.7, 17.4, 16.3, 15.5. TOF-HRMS: *m/z* $[M + H]^+$ calcd for $C_{40}H_{58}NO_3$: 600.4411; found: 600.4414.

*4.3.10. N-Phenyl (3β,20β)-3-hydroxyl-11-oxo-olean-12,30(31)-dien-32-acylhydrazine (**6j**)*. White powder, yield, 70%; m.p. 281–285°C; ^{1}H-NMR (300 MHz, $CDCl_3$), δ (ppm): 8.26 (s, 1H, NH), 7.27–7.19 (m, 2H, H-30, NH), 6.85 (m, 5H, Ar-H), 5.80 (d, 1H, *J* = 15.8 Hz, H-31), 5.67 (s, 1H, H-12), 3.23 (m, 1H, H-3), 2.77 (m, 1H, H-18), 2.34 (s, 1H, H-9), 1.38 (s, 3H), 1.13 (s, 3H), 1.12 (s, 3H), 1.00 (s, 3H), 1.01 (s, 3H), 0.81 (s, 3H), 0.80 (s, 3H); ^{13}C-NMR (75 MHz, $CDCl_3$), δ (ppm): 200.6 (C-11), 170.3 (C-13), 166.1 (C-32), 153.0 (C-30), 148.1 (C-Ar), 129.1 (2C-Ar), 128.2 (C-12), 121.1 (C-31), 119.3 (C-31), 113.8 (2C-Ar), 78.7 (C-3), 61.8 (C-9), 54.9 (C-5), 47.1 (C-18), 45.4 (C-8), 43.3, 42.3, 39.1 (2C), 37.7, 37.1, 36.8, 33.6, 32.7, 32.2, 31.0, 28.5, 28.1, 27.2, 26.39, 26.35, 23.5, 18.6, 17.4, 16.3, 15.6. TOF-HRMS: *m/z* $[M + H]^+$ calcd for $C_{38}H_{55}N_2O_3$: 587.4207; found: 587.4205.

*4.3.11. N-(4-Methyl)piperazinyl (3β,20β)-3-hydroxyl-11-oxo-olean-12,30(31)-dien-32-amide (**6k**)*. White powder, yield, 78%; m.p. 254–258°C; ^{1}H-NMR (300 MHz, $CDCl_3$), δ (ppm): 6.84 (d, 1H, *J* = 15.7 Hz, H-30), 6.19 (d, 1H, *J* = 15.7 Hz, H-31), 5.55 (s, 1H, H-12), 3.64 (m, 4H, NCH_2), 3.23 (m, 1H, H-3), 2.77 (m, 1H, H-18), 2.43 (m, 4H, NCH_2), 2.33 (s, 1H, H-9), 2.33 (s, 3H, NCH_3), 1.38 (s, 3H), 1.13 (s, 3H), 1.12 (s, 3H), 1.00 (s, 3H), 1.01 (s, 3H), 0.81 (s, 3H), 0.80 (s, 3H); ^{13}C-NMR (75 MHz, $CDCl_3$), δ (ppm): 200.2 (C-11), 169.8 (C-13), 165.6 (C-32), 152.9 (C-30), 128.3 (C-12), 118.3 (C-31), 78.7 (C-3), 61.9 (C-9), 54.9 (2C), 54.8 (C-5), 47.4 (C-18), 46.0 (2C), 45.4 (C-8), 43.4, 43.0, 39.1 (2C), 37.7, 37.1, 36.8, 33.6, 32.7, 32.3 (2×NCH_2), 31.4, 28.5, 28.1, 27.3, 26.4 (2C), 23.5, 18.7, 17.5, 16.4, 15.6 TOF-HRMS: *m/z* $[M + H]^+$ calcd for $C_{37}H_{59}N_2O_3$:

579.4520; found:579.4523.

*4.3.12. N-(4-Ethyl)piperazinyl (3β,20β)-3-hydroxyl-11-oxo-olean-12,30(31)-dien-32-amide (**6l**)*. White powder, yield, 74%; m.p. 257–262°C; ^{1}H-NMR(300 MHz, $CDCl_3$), δ (ppm): 6.84 (d, 1H, J = 15.7 Hz, H-30), 6.19 (d, 1H, J = 15.7 Hz, H-31), 5.55 (s, 1H, H-12), 3.64 (m, 4H, NCH_2), 3.23 (m, 1H, H-3), 2.77 (m, 1H, H-18), 2.45 (m, 6H, CH_2CH_3, NCH_2), 2.34 (s, 1H, H-9), 1.38 (s, 3H), 1.13 (s, 3H), 1.12 (s, 3H), 1.00 (s, 3H), 1.01 (s, 3H), 0.81 (s, 3H), 0.80 (s, 3H); ^{13}C-NMR (75 MHz, $CDCl_3$), δ (ppm): 200.2 (C-11), 169.8 (C-13), 165.5 (C-32), 152.8 (C-30), 128.3 (C-12), 118.3 (C-31), 78.7 (C-3), 61.8 (C-9), 54.9 (C-5), 52.2 (2C), 47.5 (C-18), 45.9 (2C), 45.4 (C-8), 43.3, 43.0, 39.1 (2C), 37.7, 37.1, 36.8, 33.6, 32.7, 32.3 (2C), 31.1, 28.5, 28.1, 27.3, 26.44, 26.40, 23.5, 18.7, 17.5, 16.4, 15.6, 11.8 (CH_2CH_3). TOF-HRMS: *m/z* $[M + H]^+$ calcd for $C_{38}H_{61}N_2O_3$: 593.4677; found: 593.4674.

*4.3.13. N,N-Morpholinyl (3β,20β)-3-hydroxyl-11-oxo-olean-12,30(31)-dien-32-amide (**6m**)*. White powder, yield, 76%; m.p. 265–268°C;^{1}H-NMR (300 MHz, $CDCl_3$), δ (ppm): 6.78 (d, 1H, J = 15.8 Hz, H-30), 6.57 (d, 1H, J = 7.4 Hz), 5.80 (d, 1H, J = 15.8 Hz, H-31), 5.62 (s, 1H, H-12), 4.13–3.57 (m, 4H, 2×CH_2O), 3.23 (m, 1H, H-3), 2.77 (m, 1H, H-18), 2.34 (m, 3H, H-9, NCH_2), 2.21 (m, 2H, NCH_2), 1.38 (s, 3H), 1.13 (s, 3H), 1.12 (s, 3H), 1.00 (s, 3H), 1.01 (s, 3H), 0.81 (s, 3H), 0.80 (s, 3H); ^{13}C-NMR (75 MHz, $CDCl_3$), δ (ppm): 200.2 (C-11), 169.7 (C-13), 165.8 (C-32), 153.6 (C-30), 128.3 (C-12), 117.8 (C-31), 78.7 (C-3), 66.7 ($2CH_2O$), 61.9 (C-9), 54.9 (C-5), 47.4 (C-18), 45.4 (C-8), 43.4, 43.0, 42.4, 39.1 (2C), 37.8, 37.1, 36.8, 33.5 (2C), 32.3 (2C), 31.1, 28.5, 28.1, 27.3, 26.41, 26.38, 23.5, 18.7, 17.5, 16.4, 15.6. TOF-HRMS: *m/z* $[M + H]^+$ calcd for $C_{36}H_{56}NO_4$: 566.4204; found: 566.4206.

*4.3.14. N-(3-Morpholinyl)propyl (3β,20β)-3-hydroxyl-11-oxo-olean-12,30(31)-dien-32-amide (**6n**)*. White powder,

yield, 56%; m.p. 272–276°C; ^{1}H-NMR (300 MHz, $CDCl_3$), δ (ppm): 6.89 (d, 1H, J = 4.9 Hz, NH), 6.78 (d, 1H, J = 15.8 Hz, H-30), 5.68 (d, 1H, J = 15.8 Hz, H-31), 5.55 (s, 1H, H-12), 3.73 (m, 4H, OCH_2), 3.43 (m, 4H, NCH_2), 3.23 (m, 1H, H-3), 2.78 (m, 1H, H-18), 2.49 (m, 6H, NCH_2), 2.34 (s, 1H, H-9), 1.38 (s, 3H), 1.13 (s, 3H), 1.12 (s, 3H), 1.00 (s, 3H), 1.01 (s, 3H), 0.81 (s, 3H), 0.80 (s, 3H); ^{13}C-NMR (75 MHz, $CDCl_3$), δ (ppm): 200.1 (C-11), 169.8 (C-13), 165.8 (C-32), 150.6 (C-30), 128.2 (C-12), 122.3 (C-31), 78.7 (C-3), 67.1 (2×OCH_2), 61.8 (C-9), 57.5 (2×NCH_2), 54.9 (C-5), 53.6 (2C), 47.3 (C-18), 45.4 (C-8), 43.3, 42.9, 39.1 (2C), 37.3, 37.0, 36.7, 33.5, 32.7, 32.2, 31.2, 29.7, 28.0, 27.2, 26.4, 26.3, 26.3, 25.0, 23.5, 18.6, 17.4, 16.3, 15.6. TOF-HRMS: *m/z* $[M + H]^+$ calcd for $C_{39}H_{62}NaN_2O_4$: 645.4602; found:645.4603.

*4.3.15. N-(3-Methyl)phenyl (3β,20β)-3-hydroxyl-11-oxo-olean-12,30(31)-dien-32-amide (**6o**)*. White powder, yield, 56%; m.p. 260–265°C; ^{1}H-NMR (300 MHz, $CDCl_3$), δ (ppm): 7.87 (s, 1H, NH), 7.50 (s, 1H, H-Ar), 7.44 (m, 1H, H-Ar), 7.21 (m, 1H, H-Ar), 6.95 (s, 1H, H-Ar), 6.78 (d, 1H, J = 15.8 Hz, H-30), 5.92 (d, 1H, J = 15.7 Hz, H-31) , 5.60 (s, 1H, H-12), 3.23 (m, 1H, H-3), 2.80 (m, 1H, H-18), 2.34 (s, 1H, H-9), 2.34 (s, 3H, Ar-CH_3), 1.38 (s, 3H), 1.13 (s, 3H), 1.12 (s, 3H), 1.00 (s, 3H), 1.01 (s, 3H), 0.81 (s, 3H), 0.80 (s, 3H); ^{13}C-NMR (75 MHz, $CDCl_3$), δ (ppm): 200.4 (C-11), 170.1 (C-13), 164.0 (C-32), 152.7 (C-30), 138.8 (Ar-C), 138.1 (Ar-C), 128.8 (Ar-C), 128.1 (C-12), 125.0 (Ar-C), 122.6 (Ar-C), 122.0 (C-31), 116.9 (Ar-C), 78.7 (C-3), 61.8 (C-9), 54.9 (C-5), 47.1 (C-18), 45.4 (C-8), 43.3, 42.4, 39.2, 39.1, 37.6, 37.1, 36.8, 33.8, 32.2 (2C), 31.1, 28.5, 28.1, 27.3, 26.3 (2C), 23.5, 21.5 (Ar-CH_3), 18.6, 17.4, 16.4, 15.5. TOF-HRMS: *m/z* $[M + H]^+$ calcd for $C_{39}H_{56}NO_3$: 586.4255; found:586.4253.

*4.3.16. N-Thiourea (3β,20β)-3-hydroxyl-11-oxo-olean-12,30(31)-dien-32-amide (**6p**)*. White powder, yield, 58%; m.p. 243–247°C; ^{1}H-NMR (300 MHz, DMSO-d_6), δ (ppm): 9.7 (s, 1H, NH), 6.57 (d, 1H, J = 16.0 Hz, H-30), 5.96 (s, 1H), 5.94 (d, 1H, J = 15.8 Hz, H-31), 5.68 (s, 1H, H-12), 4.31 (m, 1H), 3.02 (m, 1H, H-3), 2.59 (m, 1H,

H-18), 2.35 (s, 1H, H-9), 1.33 (s, 3H), 1.04 (s, 6H), 0.97 (s, 3H), 0.91 (s, 3H), 0.77 (s, 3H), 0.69 (s, 3H); ^{13}C-NMR (75 MHz, DMSO-d_6), δ (ppm): 200.4 (C-11), 174.8 (C=O), 169.8 (C-13), 163.9 (C-32), 155.2 (C-30), 132.7 (C-12), 126.0 (C-31), 81.8 (C-3), 66.4 (C-9), 59.3, 54.9, 51.7, 50.1, 48.2, 45.6 (2C, overlap), 42.4, 41.9 (2C), 38.0, 37.3, 37.1 (2C), 35.9, 33.6, 33.3, 32.2, 31.2 (2C), 28.5, 23.6, 21.4, 21.2. TOF-HRMS: *m/z* $[M + H]^+$ calcd for $C_{33}H_{52}N_3O_4$: 554.3952; found: 554.3955.

*4.4. General procedures for converting the carboxylic acid to an ester for compounds **7a** and **7b**.*

A solution of glycyrrhetenoic acid **5** (0.5 g, 1.0 mmol) in pyridine (2 mL) was added acetic anhydride (0.2 mL, 2.2 mmol) over 30 min, and the mixture was stirred and heated to reflux for 30 min. The reaction solution was evaporated *in vacuum*, and the residue was recrystallized from ethanol to obtain glycyrrhetenoic acid acetate (448 mg, 82%). To a solution of glycyrrhetenoic acid acetate (160 mg, 0.3 mmol,) and alcohol (10 equiv.) in CH_2Cl_2 (10 mL), was added boron trifluoride dimethyl etherate (0.7 mmol, 0.1 mL). The reaction mixture was stirred at room temperature for 24 h. The reaction mixture was added to ice-water (50 mL) and the two layers of the reaction mixture were subsequently separated. The organic layer was washed twice with water and then dried over anhydrous Na_2SO_4. The solvent was evaporated to yield a residue, which was crystallized from ethanol to obtain the esters **7a** and **7b**.

*4.4.1. Ethyl (3β,20β)-3-acetoxyl-11-oxo-olean-12,30(31)-dien-32-oate (**7a**).* White powder, yield, 77%; ^{1}H-NMR (300 MHz, $CDCl_3$), δ (ppm): 6.89 (d, 1H, J = 16.2 Hz, H-30), 5.79 (d, 1H, J = 16.2 Hz, H-31), 5.63 (s, 1H, H-12), 4.52 (m, 1H, H-3), 4.20 (q, 2H, J = 7.1 Hz, O*C*H_2CH$_3$), 2.80 (m, 1H, H-18), 2.36 (s, 1H, H-9), 2.05 (s, 3H, OAc), 1.38 (s, 3H), 1.13 (s, 3H), 1.12 (s, 3H), 1.00 (s, 3H), 1.01 (s, 3H), 0.81 (s, 3H), 0.80 (s, 3H). That is compound **4**.

*4.4.2. Benzyl (3β,20β)-3-Acetoxyl-11-oxo-olean-12,30(31)-dien-32-oate (**7b**).* White powder, yield, 73%; m.p. 243–247°C; ^{1}H-NMR (600 MHz, $CDCl_3$), δ (ppm): 7.41-7.32 (m, 5H, Ar-H), 6.95 (d, 1H, J = 16.3 Hz, H-30), 5.84 (d, 1H, J = 16.3 Hz, H-31), 5.61 (s, 1H, H-12), 5.19 (dd, 2H, J = 15.4, 12.4 Hz, O*C*H_2Ph), 4.52 (m, 1H,

3-H), 2.80 (m, 1H, H-18), 2.36 (s, 1H, H-9), 2.05 (s, 3H, Ac), 1.37 (s, 3H, H-27), 1.16 (s, 3H, H-29), 1.12 (s, 3H, H-25), 1.01 (s, 3H, H-26), 0.88 (s, 6H, H-23, H-24), 0.82 (s, 3H, H-28). TOF-HRMS: *m/z* [M + H]$^+$ calcd for $C_{41}H_{57}O_5$: 629.4201; found: 629.4198.

*4.5. Crystal structure determination for compound **6b***

X-ray single-crystal diffraction data for compound **6b** was collected on a Bruker SMART APEX CCD diffractometer at 300.79(10) K using CuK\α radiation (λ = 1.54184 Å) by the ω scan mode. The program SAINT was used for integration of the diffraction profiles. The structure was solved by direct methods using the SHELXS program of the SHELXTL package and refined by full-matrix least-squares methods with SHELXL [47]. The corrections for *LP* factors were applied. Multi-scan symmetry-related measurement was used as experimental absorption correction type. The non-hydrogen atoms of compound **6b** were refined with anisotropic thermal parameters whereas all hydrogen atoms were generated theoretically onto the parent atoms and refined isotropically with fixed thermal factors.

The crystal data of compound **6b** was as follows: Colorless block crystals, yield, 76%; mp 266-268 ^{o}C; $C_{34}H_{53}NO_3$, *Mr* = 523.77, orthorhombic, space group $P_{21\,21\,21}$; *a* = 10.0515(8), *b* = 15.1327(13), *c* = 19.9334(15) (Å); α = 90, β = 90, γ = 90, *V* = 3032.0(4) Å^3, *T* = 300.79(10), *Z* = 4, *Dx* = 1.147 g/cm^3, *F(000)* = 1152, Reflections collected / Independent reflections = 11269 / 4495, Data / restraints / parameters = 5452 / 0 / 353, Goodness of fit on F^2 =1.127, Final *R* indexes [all data], R_1 = 0.0646, $wR(F^2)$ = 0.1389.

4.6. Cell Culture

RAW264.7 murine macrophages were cultured in DMEM containing 10% fetal bovine serum, 100 units/mL penicillin, and 100 µg/mL streptomycin at 37 ºC in a 5% CO_2 humidified atmosphere.

4.7. Assay for NO Production

RAW264.7 cells were inoculated at 1×10^5 cells per well in 24-well plate and cultured for 20 h. The cells were then pre-treated with different concentrations compounds which were prepared in serum-free medium for 2 h before stimulation with LPS (1 μg/mL). After LPS-stimulated for 24 h, the NO production was determined by detecting the nitrite level using Griess reagent (Beyotime, China) according to the manufacturer's instructions, then measured absorbance of the samples at 540 nm (OD_{540}) in a microplate reader (MQX200, Bio-Tek, USA). NO inhibition rate = [control (OD_{540}) - compound (OD_{540})] / [control (OD_{540}) - blank (OD_{540})] × 100%.

Control: treated with LPS only.

Compound: treated with LPS and compounds.

Blank: cultured with fresh medium only.

4.8. Cell Cytotoxicity

Cell cytotoxicity was evaluated by methyl thiazolyl tetrazolium (MTT) assay. RAW264.7 cells were inoculated at 6×10^3 cells per well in 96-well plate. After cultured for 24 h, the cells were treated with different compounds which were diluted in DMEM for 24 h. Then 20 μL of 0.5 mg/mL MTT reagent was added into the cells and incubated for 4 h. After 4 h, cell culture was removed and then 150 μL DMSO was added to dissolve the formazan. The optical density was measured at 570 nm (OD_{570}). Cell viability was calculated from three independent experiments. The density of formazan formed in blank group was set as 100% of viability. Cell viability (%) = compound (OD_{570} / blank (OD_{570}) × 100%

Blank: cultured with fresh medium only.

Compound: treated with compounds or LPS.

4.9. Measurement of IL-6 and TNF-α

RAW264.7 cells (7×10^4 cells/well) were cultured in 24-well plate. After cultured for 24 h, and pretreated with 10μM-40 μM of compounds for 2 h, and then LPS was added. The production of IL-6 and TNF-α was stimulated by the addition of 1 μg/mL

LPS and incubated for 24 h. The levels of IL-6 and TNF-α in the supernatant were determined using the mouse ELISA kit (IL-6: R&D SYSTEMS, DY406-05. TNF-α: R&D SYSTEMS, DY410-05) which is operated according to the manufacturer's instructions. The results were analyzed using GraphPad Prism 5.0 software and SPSS version 19.0 statistic software.

4.10. Western Blot analysis

RAW264.7 cells were seeded into a 6-well culture plate at a density of 2×10^6 cells per well, and then cultured for 24 h. Then, the culture medium was replaced by fresh medium containing 10、20 and 40 μM compounds, or Bay 11-7082 (MedChemExpress, HY-13453) and 1 μg/mL LPS was added. After cultured for another 30 min or 24 h, the cells were harvested and lysed with IP buffer (Beyotime, P0013) supplemented with 1 mM phenylmethanesulfonyl fluoride (PMSF: Beyotime, ST506) and incubated on ice for 30 min. The cell lysates were centrifuged at 14,000 × g for 10 min at 4 ºC to remove insoluble materials and the supernatant was collected. Total protein concentration was determined using a BCA protein assay kit (Thermo Scientific, 23227). Each protein sample was mixed with a quarter volume of 5X SDS-PAGE sample loading buffer (100 mmol/L Tris-HCl pH 6.8, 4% SDS, 5% β-mercaptoethanol, 20% glycerol, and 0.1% bromophenol blue) and boiled for 10 min. Equal amounts of total cellular protein were loaded per well in 12.5% precast SDS-PAGE gels and then transferred to polyvinylidene difluoride membranes (Bio-Rad) for over 60 min at 300 mA. The membranes were blocked with 5% non-fat dry milk in TBS plus 0.1% Tween 20 (TBST) for 2 h at room temperature, washed 3 times in TBST for 5 min each, incubated with the primary antibody (anti-phosphorylation of SAPK/JNK, anti-SAPK/JNK, anti-phosphorylation of ERK1/2, anti-ERK1/2, anti-phosphorylation of p38, anti-p38, anti-phosphorylation of iκb, anti-iκb, antiphosphorylation of NF-kB p65, and anti-NF-κB p65) at 4 ºC overnight (all the primary antibodies were purchased from Cell Signaling Technology and diluted at the ratio of 1:1000),washed 3 times in TBST for 5 min each, incubated with anti-rabbit or anti-mouse secondary antibody (1:5000 in TBST, Cell Signaling Technology) for 90 min, washed in TBST and exposed to ECL reagents.

4.11. Immunofluorescence assay

RAW264.7 cells (7×10^4 cells/well) were cultured in 24-well plate. After cultured for 24 h, and pretreated with 20 and 40 μM of compound **6k** for 2 h, and then treated with LPS (1 μg/mL) for 3 h. The cells were washed twice with cold PBS, fixed with 4% formaldehyde for 15 min, and then permeabilized with 0.3% Triton X-100 in PBS for 10 min. After that, the cells were blocked for 0.5 h with 5% BSA. Cells were later incubated with primary antibody anti-NF-κB p65 antibody for overnight, followed by Alexa Fluor 488-labeled goat anti-rabbit IgG secondary antibody. After a wash step, stained with DAPI for 5 min and the images were acquired.

Acknowledgments

Financial support was provided by the National Natural Science Funding of China (21572003, 20802003), Anhui University Natural Science Research Project (KJ2016A339), and University Project of Introduction and Cultivation of Leading Talents (gxfxZD2016044).

Notes

The authors declare no competing financial interest.

Appendix A. Supplementary material

Crystallographic data (excluding structure factors) for the structure had been deposited with the Cambridge Crystallographic Data Center as supplementary publication No. CCDC 1418308 (**6b**). These data can be obtained free of charge via the URL http:// www.ccdc.cam.ac.uk/conts/retrieving.html (or from the CCDC, 12 Union Road, Cambridge CB2 1EZ, UK; fax: (+44) 1223 336033; e-mail: deposit@ccdc.cam.ac.uk). Representative ^{1}H and ^{13}C NMR spectra can be found at http://

References

[1] R. Medzhitov, Origin and physiological roles of inflammation, Nature 454 (2008) 428–435.

[2] R. Medzhitov, Inflammation 2010: new adventures of an old flame, Cell 140 (2010) 771–776.

[3] Y.C. Lee, C.H. Chang, J.W. Lin, H.C. Chen, M.S. Lin, M.S. Lai, Non-steroidal anti-inflammatory drugs use and risk of upper gastrointestinal adverse events in cirrhotic patients, Liver Int. 32 (2012) 859–866.

[4] C. Pereira-Leite, C. Nunes, S.K. Jamal, I.M. Cuccovia, S. Reis, Nonsteroidal anti-inflammatory therapy: a journey toward safety. Med. Res. Rev. 37 (2017) 802–859.

[5] E. Patridge, P. Gareiss, M.S. Kinch, D. Hoyer, An analysis of FDA-approved drugs: natural products and their derivatives, Drug Discov. Today 21 (2016) 204–207.

[6] R. Gautam, S.M. Jachak, Recent developments in anti-inflammatory natural products, Med. Res. Rev. 29 (2009) 767–820.

[7] M.N. Asl, H. Hosseinzadeh, Review of pharmacological effects of *Glycyrrhiza* sp. and its bioactive compounds, Phytother. Res. 22 (2008) 709–724.

[8] J.K. Kim, S.M. Oh, H.S. Kwon, Y.S. Oh, S.S. Lim, H. K. Shin, Anti-inflammatory effect of roasted licorice extracts on lipopolysaccharide-induced inflammatory responses in murine macrophages, Biochem. Biophys. Res. Commun. 345 (2006) 1215–1223.

[9] C. Fiore, M. Eisenhut, R. Krausse, E. Ragazzi, D. Pellati, D. Armanini, J. Bielenberg, Antiviral effects of *Glycyrrhiza* species, Phytother. Res. 22 (2008) 141–148.

[10] W.J. Tang, Y.A. Yang, H. Xu, J.B. Shi, X.H. Liu, Synthesis and discovery of 18α-GAMG as anticancer agent *in vitro* and *in vivo via* down expression of protein p65, Sci. Rep. 4 (2014) 7106.

[11] T.C. Kao, M.H. Shyu, G.C. Yen, Glycyrrhizic acid and 18beta-glycyrrhetic acid inhibit inflammation via P13k/Akt/GSK3beta signaling and glucocorticoid receptor activation, J. Agric. Food Chem. 58 (2010) 8623–8629.

[12] M.N. Oztanir, O. Ciftci, A. Cetin, M.A. Durak, N. Basak, Y. Akyuva, The beneficial effects of 18β-glycyrrhetic acid following oxidative and neuronal damage in brain tissue caused by global cerebral ischemia/reperfusion in a C57BL/J6 mouse model, Neurol. Sci. 35 (2014) 1221–1228.

[13] G. Hoever, L. Baltina, M. Michaelis, R. Kondratenko, L. Baltina, G.A. Tolstikov, H.W. Doerr, J. Jr. Cinatl, Antiviral activity of glycyrrhizic acid derivatives against SARS-coronavirus, J. Med. Chem. 48 (2005) 1256–1259.

[14] K. Oyama, M. Kawada-Matsuo, Y. Oogai, T. Hayashi, N. Nakamura, H. Komatsuzawa, Antibacterial effects of glycyrrhetic acid and its derivatives on *Staphylococcus aureus*, PLoS One. 11 (2016) e0165831.

[15] X. Wu, L. Zhang, E. Gurley, E. Studer, J. Shang, T. Wang, C. Wang, M. Yan, Z. Jiang, P.B. Hylemon, A.J. Sanyal, W.M. Jr. Pandak, H. Zhou, Prevention of free fatty acid-induced hepatic lipotoxicity by 18beta-glycyrrhetic acid through lysosomal and mitochondrial pathways, Hepatology 47 (2008) 1905–1915.

[16] C.Y. Wang, T.C. Kao, W.H. Lo, G.C. Yen, Glycyrrhizic acid and 18β-glycyrrhetic acid modulate lipopolysaccharide-induced inflammatory response by suppression of NF-κB through PI3K p110δ and p110γ inhibitions, J. Agric. Food Chem. 59 (2011) 7726–7733.

[17] Y. Xiao, J. Xu, C. Mao, M. Jin, Q. Wu, J. Zou, Q. Gu, Y. Zhang, Y. Zhang, 18Beta-glycyrrhetic acid ameliorates acute propionibacterium acnes-induced liver injury through inhibition of macrophage inflammatory protein-1alpha, J. Biol. Chem. 285 (2010) 1128–1137.

[18] N. Bordbar, M.H. Karimi, Z. Amirghofran, Phenotypic and functional maturation of murine dendritic cells induced by 18alpha- and beta-glycyrrhetic acid, Immunopharmacol. Immunotoxicol. 36 (2014) 52–60.

[19] O. Robles, D. Romo, Chemo- and site-selective derivatizations of natural products enabling biological studies, Nat. Prod. Rep. 31 (2014) 318–334.

[20] J. Chen, W. Li, H. Yao, J. Xu, Insights into drug discovery from natural products through structural modification, Fitoterapia 103 (2015) 231–241.

[21] H. Yao, J. Liu, S. Xu, Z. Zhu, J. Xu, The structural modification of natural products for novel drug discovery, Expert. Opin. Drug Discov. 12 (2017) 121–140.

[22] H. Inoue, T. Mori, S. Shibata, Y. Koshihara, Modulation by glycyrrhetic acid derivatives of TPA-induced mouse ear oedema, Br. J. Pharmacol. 96 (1989) 204–210.

[23] H. Inoue, K. Inoue, T. Takeuchi, N. Nagata, S. Shibata, Inhibition of rat acute inflammatory paw oedema by dihemiphthalate of glycyrrhetic acid derivatives: comparison with glycyrrhetic acid, J. Pharm. Pharmacol. 34 (1993) 1067–1071.

[24] R. Csuk, S. Schwarz, R. Kluge, D. Ströhl, Synthesis and biological activity of some antitumor active derivatives from glycyrrhetic acid, Eur. J. Med. Chem. 45 (2010) 5718–5723.

[25] R. Csuk, S. Schwarz, B. Siewert, R. Kluge, D. Strohl, Synthesis and antitumor activity of ring A modified glycyrrhetic acid derivatives, Eur. J. Med. Chem. 46 (2011)

5356–5369.

[26] E.B. Logashenko, O.V. Salomatina, A.V. Markov, D.V. Korchagina, N.F. Salakhutdinov, G.A. Tolstikov, V.V. Vlassov, M.A. Zenkova, Synthesis and pro-apoptotic activity of novel glycyrrhetic acid derivatives, ChemBioChem, 12 (2011) 784–794.

[27] O.V. Salomatina, A.V. Markov, E.B. Logashenko, D.V. Korchagina, M.A. Zenkova, N.F. Salakhutdinov, V.V. Vlassov, G.A. Tolstikov, Synthesis of novel 2-cyano substituted glycyrrhetic acid derivatives as inhibitors of cancer cells growth and NO production in LPS-activated J-774 cells, Bioorg. Med. Chem. 22 (2014) 585–593.

[28] A.T. Dinkova-Kostova, P. Talalay, Direct and indirect antioxidant properties of inducers of cytoprotective proteins, Mol. Nutr. Food Res. 52 (2008) S128−S138.

[29] J. Krysiak, R. Breinbauer, Activity-based protein profiling for natural product target discovery, Top. Curr. Chem. 324 (2012) 43−84.

[30] L. Arshad, I. Jantan, S.N. Bukhari, M.A. Haque, Immunosuppressive effects of natural α,β-unsaturated carbonyl-based compounds, and their analogs and derivatives, on immune cells: a review, Front Pharmacol. 8 (2017) 22.

[31] M.B. Sporn, K.T. Liby, M.M. Yore, L. Fu, J.M. Lopchuk, G.W. Gribble, New synthetic triterpenoids: potent agents for prevention and treatment of tissue injury caused by inflammatory and oxidative stress, J. Nat. Prod. 74 (2011) 537−745.

[32] R. You, W. Long, Z. Lai, L. Sha, K. Wu, X. Yu, Y. Lai, H. Ji, Z. Huang, Y. Zhang, Discovery of a potential anti-inflammatory agent: 3-oxo-29-noroleana-1,9(11),12-trien-2,20-dicarbonitrile, J. Med. Chem. 56 (2013) 1984−1995.

[33] D. Du, J. Yan, J. Ren, H. Lv, Y. Li, S. Xu, Y. Wang, S. Ma, J. Qu, W. Tang, Z. Hu, S. Yu, Synthesis, biological evaluation, and molecular modeling of glycyrrhizin derivatives as potent high-mobility group box-1 inhibitors with anti-heart-failure activity *in vivo*, J. Med. Chem. 56 (2013) 97−108.

[34] L.A. Baltina, Chemical modification of glycyrrhizic acid as a route to new bioactive compounds for medicine. Curr. Med. Chem. 10 (2003) 155−171.

[35] F. Aktan, iNOS-mediated nitric oxide production and its regulation, Life Sci. 75 (2004) 639–653.

[36] B. Li, Y.A. Yang, L.Z. Chen, S.C. Chen, J. Zhang, W.J. Tang, 18α-Glycyrrhetinic acid monoglucuronide as an anti-inflammatory agent through

suppression of the NF-κB and MAPK signaling pathway, Med. Chem. Commun. 8 (2017) 1498–1504.

[37] D.M. Mosser, J.P. Edwards, Exploring the full spectrum of macrophage activation, Nat. Rev. Immunol. 8 (2008) 958–969.

[38] C. Tsatsanis, A. Androulidaki, M. Venihaki, A.N. Margioris, Signalling networks regulating cyclooxygenase-2, Int. J. Biochem. Cell Biol. 38 (2006) 1654–1661.

[39] T. Lawrence, The nuclear factor NF-kappaB pathway in inflammation, Cold Spring Harb. Perspect. Biol. 1 (2009) a001651.

[40] M. Karin, Y. Ben-Neriah, Phosphorylation meets ubiquitination: the control of NF-[kappa]B activity, Annu. Rev. Immunol. 18 (2000) 621–663.

[41] L.Z. Chen, W.W. Sun, L. Bo, J.Q. Wang, C. Xiu, W.J. Tang, J.B. Shi, H.P. Zhou, X.H. Liu, New arylpyrazoline-coumarins: Synthesis and anti-inflammatory activity, Eur. J. Med. Chem. 138 (2017) 170–181.

[42] G. Pearson, F. Robinson, T. Beers Gibson, B.E. Xu, M. Karandikar, K. Berman, M.H. Cobb, Mitogen-activated protein (MAP) kinase pathways: regulation and physiological functions, Endocr. Rev. 22 (2) (2001) 153–183.

[43] S. Ghosh, M. S. Hayden, New regulators of NF-kappaB in inflammation, Nat. Rev. Immunol. 8 (2008) 837–848.

[44] D.W. Hommes, M.P. Peppelenbosch, S.J. van Deventer, Mitogen activated protein (MAP) kinase signal transduction pathways and novel anti-inflammatory targets, Gut 52 (2003) 144–151.

[45] R. Doi, M. Shibuya, T. Murayama, Y. Yamamoto, Y. Iwabuchi, Development of an azanoradamantane-type nitroxyl radical catalyst for class-selective oxidation of alcohols, J. Org. Chem. 80 (2015) 401–113.

[46] W.S. Wadsworth, W.D. Emmons, Ethyl cyclohexenylacetate, Org. Synth. 5 (1973) 547; 45 (1965) 44.

[47] G.M. Sheldrick, SHELXTL-97, Program for crystal structure solution and refinement, University of Göttingen, Göttingen, Germany, 1997.

Figure Captions

Table 1

Effect of glycyrrhetin derivatives on the viability of RAW264.7 cells[a]

Fig. 1. The general design strategy in this study.

Fig. 2. ORTEP drawing of compound **6b**.

Fig. 3. The inhibitory effects of glycyrrhetin derivatives on NO production in LPS-stimulated RAW 264.7 cells. RAW 264.7 cells were pretreated with glycyrrhetin derivatives (**A**: 40μM and **B**: 20μM) for 2 h, and then in the presence or absence of LPS (1 μg/mL) for 24 h. The results were showed as means ± SD (n = 3) of at least three independent experiments.$^{\#}$ $p < 0.05$, $^{\#\#}$ $p < 0.01$, $^{\#\#\#}$ $p < 0.001$ compared with the blank group; * $p < 0.05$, ** $p < 0.01$, *** $p < 0.001$ compare with LPS-stimulated group.

Fig. 4. Compounds **6k** and **6l** inhibited LPS-induced IL-6 and TNF-α production in RAW264.7 cells (**A** and **B**). RAW 264.7 cells were incubated with different concentrations of compounds **6k** and **6l** for 2 h, and then in the presence or absence of LPS (1 μg/mL) for 24 h. $^{\#}$ $p < 0.05$, $^{\#\#}$ $p < 0.01$, $^{\#\#\#}$ $p < 0.001$ compared with the control group; * $p < 0.05$, ** $p < 0.01$, *** $p < 0.001$ compare with LPS-stimulated group.

Fig. 5. Effects of compound **6k** on LPS-induced iNOS and COX-2 protein expression in RAW264.7 cells. The cells were treated with different concentrations of compound **6k**, and then in the presence or absence of LPS (1 μg/mL) for 24 h. Bay 11-7082 is the NF-κB inhibitors (20 μM). The results were showed as means ± SD (n = 3) of at least three independent experiments. $^{\#}$ $p < 0.05$, $^{\#\#}$ $p < 0.01$, $^{\#\#\#}$ $p < 0.001$ compared with the control group; * $p < 0.05$, ** $p < 0.01$, *** $p < 0.001$ compare with LPS-stimulated group.

Fig. 6. A: Compound **6k** suppressed LPS-induced activation of NF-κB signaling pathway in RAW 264.7 cells. RAW264.7 cells were treated with compound **6k** (10 μM – 40 μM) and LPS (1 μg/mL) for 30 min. The levels of NF-κB p65, IκB, and their phosphorylated forms were analyzed using western blotting. Bay 11-7082 is the NF-κB inhibitors (20 μM). The results were showed as means ± SD (n = 3) of at least three independent experiments. $^{\#}p < 0.05$, $^{\#\#\#}p < 0.01$, $^{\#\#\#}p < 0.001$ compared with the control group; $^{*}p < 0.05$, $^{**}p < 0.01$, $^{***}p < 0.001$ compared with LPS-stimulated group.

B: Compound **6k** clearly inhibited NF-κB p65 nuclear translocation. RAW264.7 were pretreated with compound **6k** for 1 h and then stimulated with LPS (1 μg/mL) for 3 h.

Fig. 7. Compound **6k** suppressed LPS-induced activation of MAPK signaling pathway in RAW 264.7 cells. RAW264.7 cells were treated with Compound **6k** (10 μM – 40 μM) and LPS (1 μg/mL) for 30 min. The levels of JNK, ERK1/2, and p38 MAPK proteins, and their phosphorylated forms were analyzed using western blotting. The results were showed as means ± SD (n = 3) of at least three independent experiments. $^{\#}p < 0.05$, $^{\#\#\#}p < 0.01$, $^{\#\#\#}p < 0.001$ compared with the control group; $^{*}p < 0.05$, $^{**}p < 0.01$, $^{***}p < 0.001$ compared with LPS-stimulated group.

Scheme 1. Synthesis of compound **5**.

Scheme 2. Synthesis of glycyrrhetenoic acid derivatives **6a**–**6p**.

Scheme 3. Synthesis of glycyrrhetenoic acid derivatives **7a**–**7b**.

Table 1

Effect of glycyrrhetin derivatives on the viability of RAW264.7 cells[a]

Compound	Concentration	Cell viability (%)[a]	Compound	Concentration	Cell viability (%)[a]
blank		100	**6g**	20μM	95.8±4.0
LPS	1μg/mL	98.5±3.8	**6i**	20μM	93.0±4.5
GA	40μM	101.8±5.3	**6j**	20μM	94.8±4.1
5	40μM	99.2±4.6	**6k**	40μM	96.6±6.7
6a	40μM	100.4±4.8	**6l**	40μM	98.4±4.0
6b	40μM	99.5±4.2	**6m**	40μM	97.5±5.6
6c	40μM	92.0±6.2	**6n**	40μM	99.8±2.4
6d	20μM	93.6±2.7	**6o**	40μM	99.3±3.6
6e	20μM	91.4±3.2	**6p**	20μM	96.7±4.5
6f	40μM	97.6±3.2	**7a**	20μM	94.3±3.1
6h	40μM	95.0±5.1	**7b**	20μM	96.9±6.2

[a] The results were showed as means ± SD of at least three independent experiments.

Fig. 1. The general design strategy in this study.

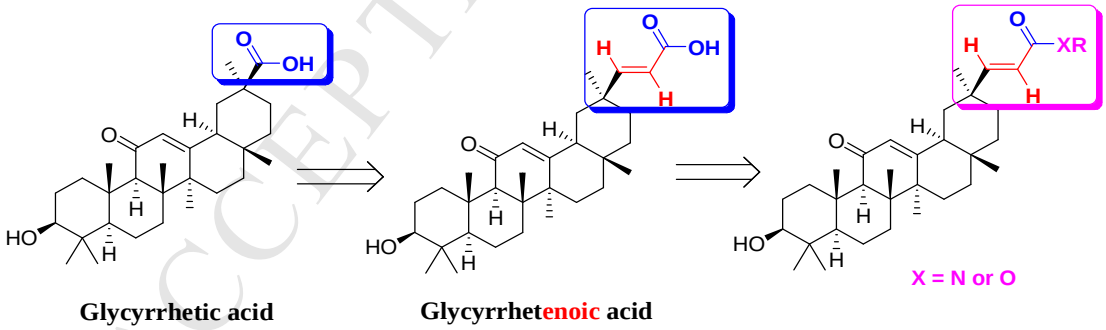

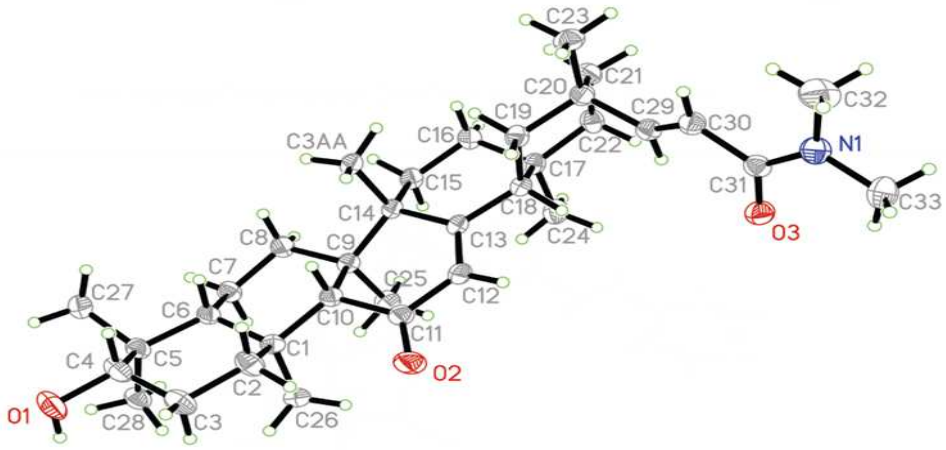

Fig. 2. ORTEP drawing of compound **6b**.

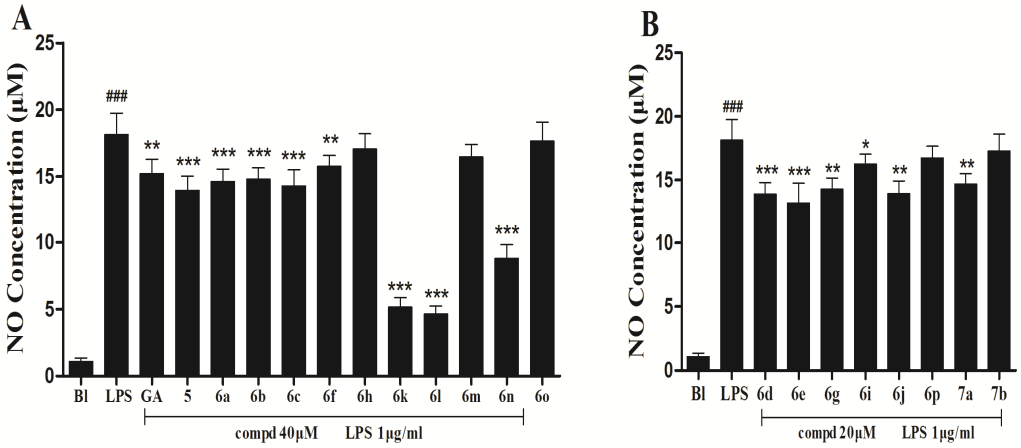

Fig. 3. The inhibitory effects of glycyrrhetin derivatives on NO production in LPS-stimulated RAW 264.7 cells. RAW 264.7 cells were pretreated with glycyrrhetin derivatives (**A**: 40μM and **B**: 20μM) for 2 h, and then in the presence or absence of LPS (1 μg/mL) for 24 h. The results were showed as means ± SD (n = 3) of at least three independent experiments.$^{\#}$ $p < 0.05$, $^{\#\#}$ $p < 0.01$, $^{\#\#\#}$ $p < 0.001$ compared with the blank group; * $p < 0.05$, ** $p < 0.01$, *** $p < 0.001$ compare with LPS-stimulated group.

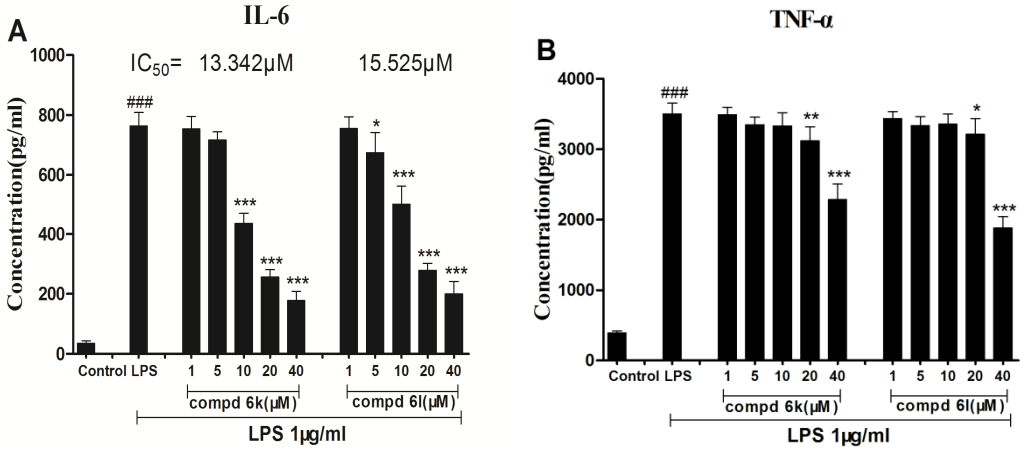

Fig. 4. Compounds **6k** and **6l** inhibited LPS-induced IL-6 and TNF-α production in RAW264.7 cells (**A** and **B**). RAW 264.7 cells were incubated with different concentrations of compounds **6k** and **6l** for 2 h, and then in the presence or absence of LPS (1 μg/mL) for 24 h. $^{\#}p < 0.05$, $^{\#\#}p < 0.01$, $^{\#\#\#}p < 0.001$ compared with the control group; $^{*}p < 0.05$, $^{**}p < 0.01$, $^{***}p < 0.001$ compare with LPS-stimulated group.

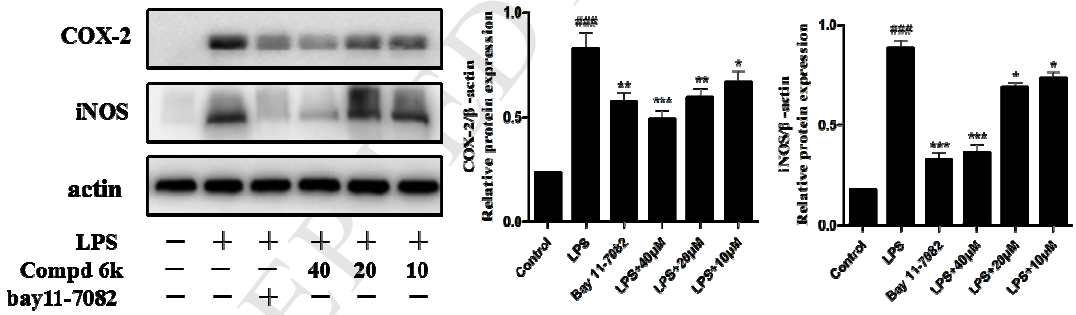

Fig. 5. Effects of compound **6k** on LPS-induced iNOS and COX-2 protein expression in RAW264.7 cells. The cells were treated with different concentrations of compound **6k**, and then in the presence or absence of LPS (1 μg/mL) for 24 h. Bay 11-7082 is the NF-κB inhibitors (20 μM). The results were showed as means ± SD (n = 3) of at least three independent experiments. $^{\#}p < 0.05$, $^{\#\#}p < 0.01$, $^{\#\#\#}p < 0.001$ compared with the control group; $^{*}p < 0.05$, $^{**}p < 0.01$, $^{***}p < 0.001$ compare with LPS-stimulated group.

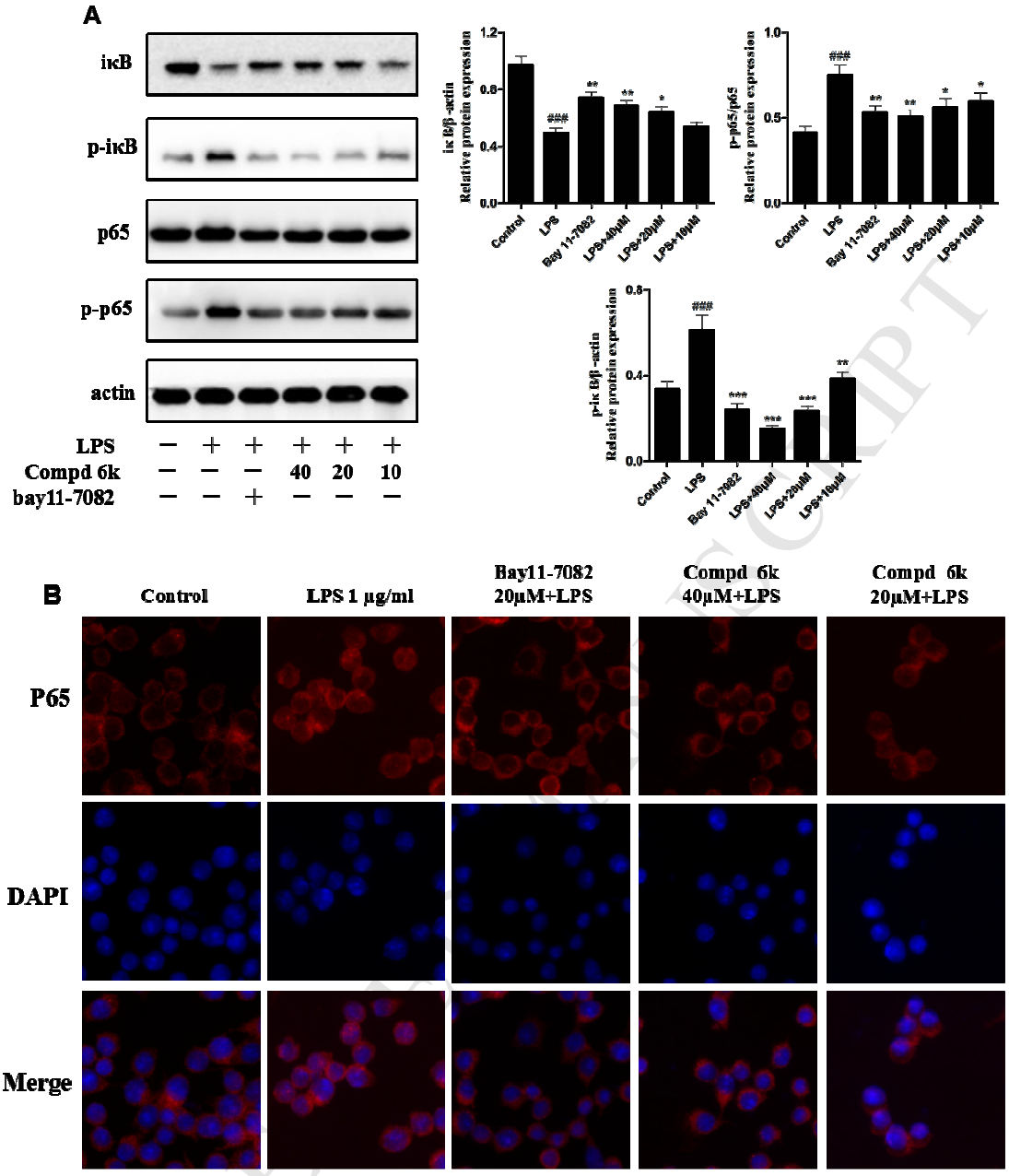

Fig. 6. A: Compound **6k** suppressed LPS-induced activation of NF-κB signaling pathway in RAW 264.7 cells. RAW264.7 cells were treated with compound **6k** (10 μM – 40 μM) and LPS (1 μg/mL) for 30 min. The levels of NF-κB p65, IκB, and their phosphorylated forms were analyzed using western blotting. Bay 11-7082 is the NF-κB inhibitors (20 μM). The results were showed as means ± SD (n = 3) of at least three independent experiments. $^{\#}p < 0.05$, $^{\#\#\#}p < 0.01$, $^{\#\#\#}p < 0.001$ compared with the control group; $^{*}p < 0.05$, $^{**}p < 0.01$, $^{***}p < 0.001$ compared with LPS-stimulated group.

B: Compound **6k** clearly inhibited NF-κB p65 nuclear translocation. RAW264.7 were

pretreated with compound **6k** for 1 h and then stimulated with LPS (1 μg/mL) for 3 h.

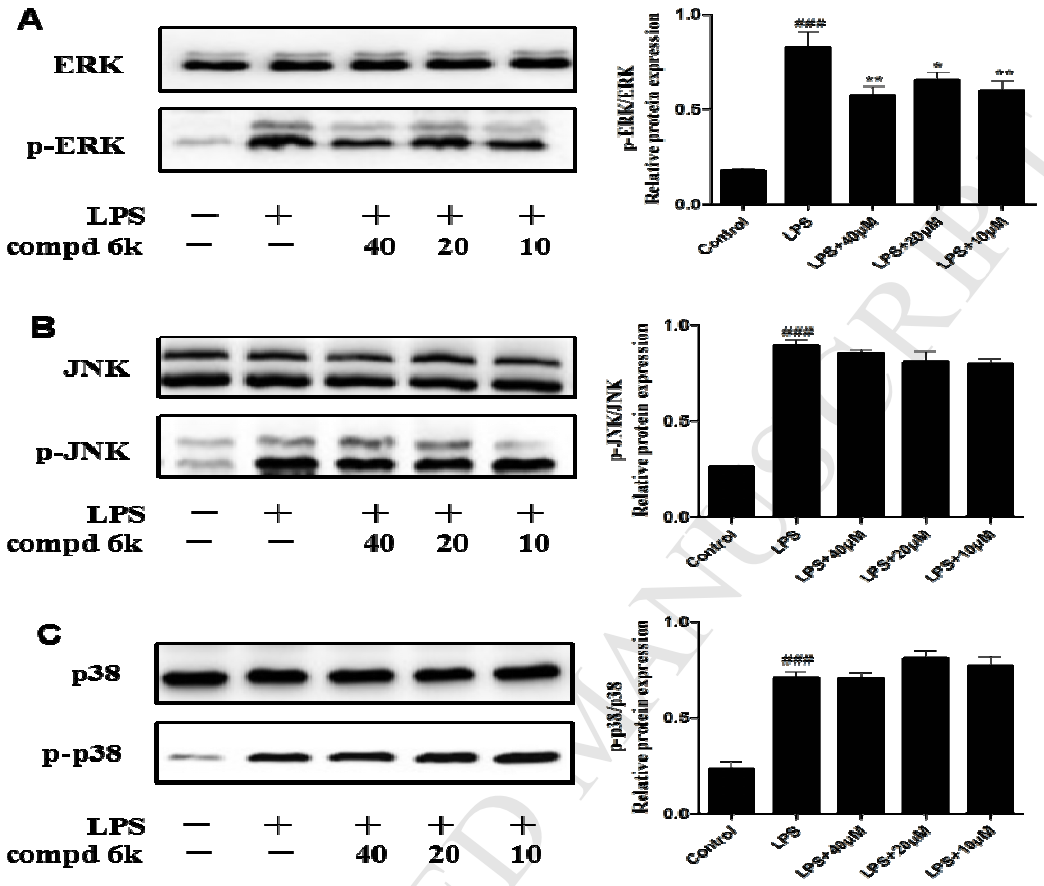

Fig. 7. Compound **6k** suppressed LPS-induced activation of MAPK signaling pathway in RAW 264.7 cells. RAW264.7 cells were treated with Compound **6k** (10 μM – 40 μM) and LPS (1 μg/mL) for 30 min. The levels of JNK, ERK1/2, and p38 MAPK proteins, and their phosphorylated forms were analyzed using western blotting. The results were showed as means ± SD (n = 3) of at least three independent experiments. $^{\#}p < 0.05$, $^{\#\#\#}p < 0.01$, $^{\#\#\#}p < 0.001$ compared with the control group; $^{*}p < 0.05$, $^{**}p < 0.01$, $^{***}p < 0.001$ compared with LPS-stimulated group.

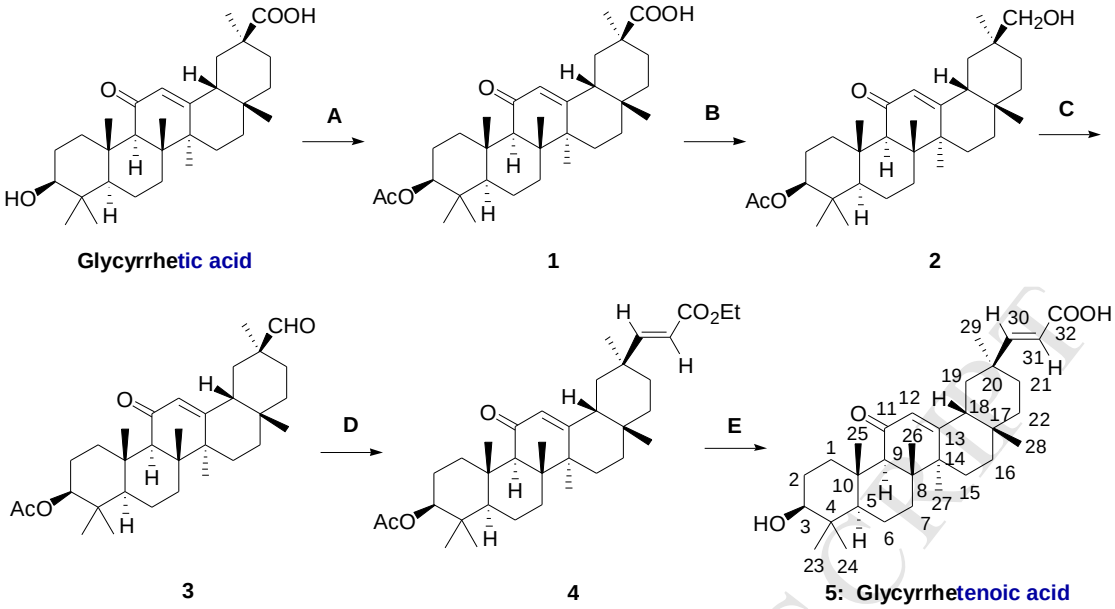

Scheme 1. Synthesis of compound **5**.

Reagents and conditions: (**A**) Ac_2O-C_5H_5N, rt, 4h; (**B**) $ClCOOC_2H_5$, NEt_3, THF, -5ºC, 30min: $NaBH_4$, H_2O, rt, 4h; (**C**) PCC, CH_2Cl_2, 0°C, rt, 2h; (**D**) NaH, $(EtO)_2P(O)CH_2CO_2Et$, THF, 0°C, rt, 3h; (**E**) 5% NaOH, rt, 2h.

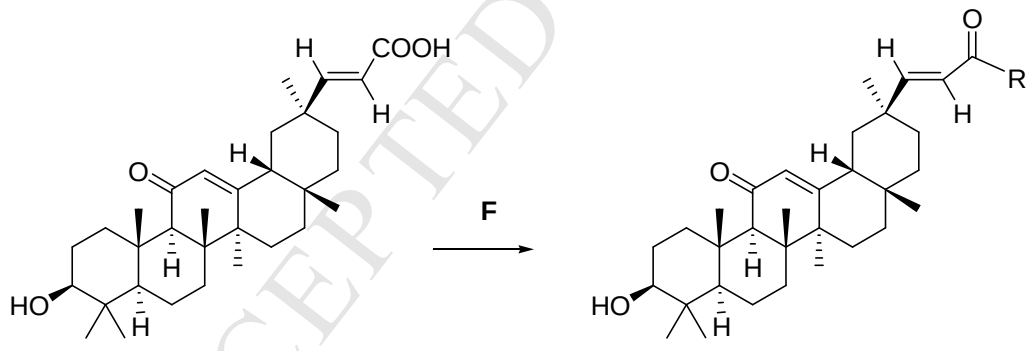

R = $-NHCH_3$ **6a**; $-N(CH_3)_2$ **6b**; $-NHCH_2CH_3$ **6c**; $-NH(CH_2)_2OH$ **6d**; $-NHCH_2CHMeOH$ **6e**; $-NHi\text{-}Pr$ **6f**; $-N(i\text{-}Pr)_2$ **6g**; $-NH(CH_2)_3Cl$ **6h**; $-NH(CH_2)_2Ph$ **6i**; $-NHNHPh$ **6j**; 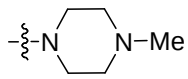 **6k**; 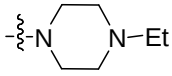 **6l**; 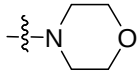 **6m**; 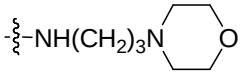 **6n**; 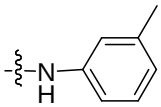 **6o**; 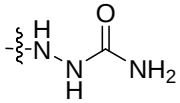 **6p**

Scheme 2. Synthesis of glycyrrhetenoic acid derivatives **6a**–**6p**.

Reagents and conditions: (**F**) EDC·HCl, HOBt, NEt_3, CH_2Cl_2.

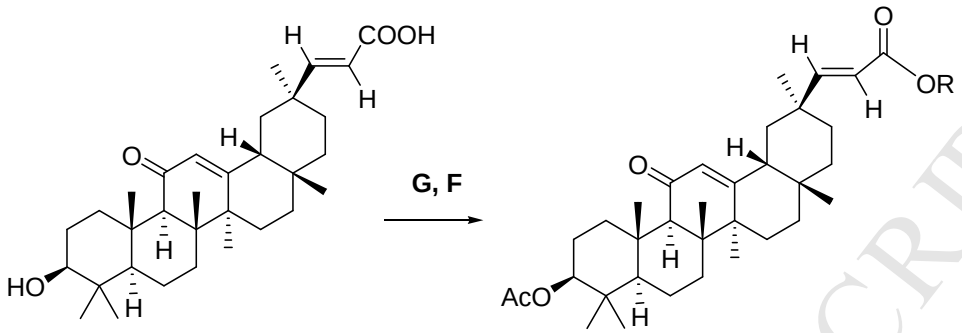

5 **7**

7a: R = CH_2CH_3; **7b:** R = CH_2Ph

Scheme 3. Synthesis of glycyrrhetenoic acid derivatives **7a**–**7b**.

Reagents and conditions: (**G**) Ac_2O, Pyridine; (**F**) BF_3·THF, R-OH, CH_2Cl_2.

Highlights

- The unsaturated carbonyl unit improved activity of Glycyrrhetic acid.
- Piperazine unit increases anti-inflammatory activity of compound **5**.
- **6k** and **6l** could suppress iNOS, COX-2 expression and NO, IL-6 production.
- The mechanism of **6k** was through MAPKs and NF-kB signaling pathway.